CONFIDENTIAL

NACA RM L54K08

NACA

RESEARCH MEMORANDUM

THEORETICAL ANALYSIS OF THE LONGITUDINAL BEHAVIOR OF AN AUTOMATICALLY CONTROLLED SUPERSONIC INTERCEPTOR DURING THE ATTACK PHASE

By Ordway B. Gates, Jr., and C. H. Woodling

Langley Aeronautical Laboratory
Langley Field, Va.

CLASSIFIED DOCUMENT

This material contains information affecting the National Defense of the United States within the meaning of the espionage laws, Title 18, U.S.C., Secs. 793 and 794, the transmission or revelation of which in any manner to an unauthorized person is prohibited by law.

NATIONAL ADVISORY COMMITTEE
FOR AERONAUTICS

WASHINGTON

January 28, 1955

CONFIDENTIAL

[redacted]

NATIONAL ADVISORY COMMITTEE FOR AERONAUTICS

RESEARCH MEMORANDUM

THEORETICAL ANALYSIS OF THE LONGITUDINAL BEHAVIOR OF AN AUTOMATICALLY CONTROLLED SUPERSONIC INTERCEPTOR DURING THE ATTACK PHASE

By Ordway B. Gates, Jr., and C. H. Woodling

SUMMARY

A theoretical analysis has been made of the longitudinal behavior of an automatically controlled supersonic interceptor during the attack phase. The control system used to control the interceptor's flight path was one in which a pitching velocity was commanded proportional to the longitudinal tracking error. Throughout the investigation the assumption is made that the target is flying on a straight-line path.

Factors considered in this investigation included effects of control-system parameters, effects of limitations on control deflection and rate of control deflection, effects of initial tracking errors, effects of nonlinear variations in drag and lift with angle of attack and Mach number, effects of nonlinear variations in pitching moment with angle of attack, effect of variations in interceptor forward velocity, and the effect of a normal acceleration limiter on the system performance.

The control system considered in this investigation was found to give acceptable control of the interceptor's flight path during attack runs against a nonmaneuvering target.

The inclusion of a nonlinear variation of drag and lift with angle of attack and Mach number resulted in relatively large variations in the interceptor forward velocity during the attack runs. However, the effects of velocity changes on the overall responses during the attack runs were considerably reduced when a signal proportional to the change in forward velocity was fed back to the elevator servo.

INTRODUCTION

The Langley Laboratory of the National Advisory Committee For Aeronautics is presently engaged in an interceptor research program, one

[redacted]

of the purposes of which is to evaluate the tracking performance of a supersonic interceptor equipped with various types of automatic control systems. The present paper is concerned with an analysis of that phase of the problem wherein the interceptor's radar locks on, with an initial vertical tracking error, to a bomber flying at a constant velocity; only maneuvers of the interceptor in the vertical plane are required to carry out the interception. The results obtained from analysis of this longitudinal phase of the general tracking problem are intended to provide information which will be useful in the synthesis of a satisfactory longitudinal control system for the interceptor being studied. The interceptor considered in this investigation is similar to that analyzed in reference 1, which has a notched delta wing of aspect ratio 3.2 and 55° sweepback of the leading edge.

For this investigation the interceptor is assumed to be flying initially in level flight at a Mach number of 2.2 at an altitude of 50,000 feet and the target is flying in level flight toward the interceptor at a Mach number of 1.4, at various altitudes above 50,000 feet. No consideration was given to the effects of altitude changes on the interception problem discussed in this paper.

The guidance equations presented in this paper are for a lead-collision type of navigation.

The results of this investigation are presented, for the most part, in the form of interceptor and kinematic responses subsequent to radar lock-on, which were computed on the Reeves Electronic Analog Computer (REAC).

SYMBOLS

I_Y	moment of inertia about Y stability axis, slug-ft^2
m	mass of airplane, slugs
$\bar{c}$	mean aerodynamic chord, ft
S	wing area, sq ft
q	dynamic pressure, lb/sq ft
V	forward velocity, ft/sec
M	Mach number
n	normal acceleration, g units

[redacted]

g acceleration due to gravity, ft/sec^2

q $\dot{\theta}\bar{c}/2V$ when used as a subscript

θ angle of pitch, radians unless otherwise specified

α angle of attack, radians unless otherwise specified

γ flight-path angle ($\gamma = \theta - \alpha$), radians unless otherwise specified

u change in forward velocity, ft/sec

u' relative change in forward velocity, $\frac{u}{V}$

δ_e elevator deflection, radians unless otherwise specified

$\delta_e' = -\delta_e$

t time, sec

C_L trim lift coefficient, $\frac{\text{Lift}}{qS}$

C_D trim drag coefficient, $\frac{\text{Drag}}{qS}$

C_m pitching-moment coefficient, $\frac{\text{Pitching moment}}{qS\bar{c}}$

$C_{L_{\delta_e}} = \frac{\partial C_L}{\partial \delta_e}$, per radian

$C_{L_\alpha} = \frac{\partial C_L}{\partial \alpha}$, per radian

$C_{m_{\delta_e}} = \frac{\partial C_m}{\partial \delta_e}$, per radian

$C_{m_\alpha} = \frac{\partial C_m}{\partial \alpha}$, per radian

[redacted]

$$C_{m_{\dot{\alpha}}} = \frac{\partial C_m}{\partial \frac{\dot{\alpha}\bar{c}}{2V}}, \text{ per radian}$$

$$C_{m_q} = \frac{\partial C_m}{\partial \frac{\dot{\theta}\bar{c}}{2V}}, \text{ per radian}$$

$$C_{m_{u'}} = \frac{\partial C_m}{\partial \left(\frac{u}{V}\right)}, \text{ per radian}$$

$$C_{D_\alpha} = \frac{\partial C_D}{\partial \alpha}, \text{ per radian}$$

D differential operator, $\frac{d}{dt}$

σ angle between interceptor X body axis and radar line of sight, positive when line of sight is above body axis, radians unless otherwise specified

R distance from interceptor to target along line of sight, measured positive from interceptor to target, ft

Ω angular velocity of line of sight, $(\Omega = \dot{\sigma} + \dot{\theta})$, radians/sec; positive when line of sight is rotating upward

t_G time of flight of interceptor from instantaneous position to firing point, sec

τ time of flight of interceptor's rockets from firing point to predicted point of contact with target, sec

$\bar{M}$ predicted miss distance, measured positive from interceptor to target, ft

M_{LS} component of $\bar{M}$ along the instantaneous line of sight, positive when target is ahead of rockets at predicted time of impact, ft

M_{NLS} component of $\bar{M}$ perpendicular to the instantaneous line of sight, positive when target is below rockets at predicted time of impact, ft

[redacted]

ϵ_γ error in interceptor's flight path at any given instant,

$$\epsilon_\gamma \approx - \frac{M_{NLS}}{V_I t_G + \left(V_I + V_R\right)\tau}$$

τ_s elevator servo-system time constant, sec

ϵ_f output of filter, radians

τ_f filter time constant, sec

K tracking-loop gain constant, radians/sec/radian

K_r rate of pitch-feedback gain, radians/sec/radians/sec

K_s elevator-servo gain constant, radians/radian/sec

Subscripts:

I interceptor

R rocket

T target

L limit

ss steady state

i input

o initial value

ANALYSIS

Derivation of Guidance Equations

The type of navigation or interception considered in this investigation is lead collision; that is, the interceptor endeavors to fly a constant flight path such that at only one point on the path the rockets of the interceptor may be fired and a hit obtained on the target. The rockets, subsequent to firing, fly a constant bearing course with the target to the predicted point of impact. The geometry of the attack

[redacted]

problem is shown diagrammatically in figure 1. Generally, the vector equation which must be satisfied is:

$$\bar{R} + \overline{V_T\left(t_G + \tau\right)} = \overline{V_I t_G + \left(V_I + V_R\right)\tau} + \bar{M} \tag{1}$$

The components of this vector equation along and normal to the instantaneous line of sight are:

$$\left.\begin{aligned} R + V_T\left(t_G + \tau\right)\cos\left(\sigma + \theta - \gamma_T\right) &= \left[V_I t_G + \left(V_I + V_R\right)\tau\right]\cos(\sigma + \alpha) + M_{LS} \\ V_T\left(t_G + \tau\right)\sin\left(\sigma + \theta - \gamma_T\right) &= \left[V_I t_G + \left(V_I + V_R\right)\tau\right]\sin(\sigma + \alpha) + M_{NLS} \end{aligned}\right\} \tag{2}$$

The target flight-path angle γ_T is taken as zero when the target is in level flight going away from the interceptor and is taken as π when in level flight coming toward the interceptor. The equations may be rewritten in terms of the range, rate of change of range, and angular velocity of the line of sight as:

$$\left.\begin{aligned} R + \dot{R}\left(t_G + \tau\right) - V_R\tau\cos(\sigma + \alpha) &= M_{LS} \\ -R\Omega\left(t_G + \tau\right) - V_R\tau\sin(\sigma + \alpha) &= M_{NLS} \end{aligned}\right\} \tag{3}$$

where

$$\dot{R} = V_T\cos\left(\sigma + \theta - \gamma_T\right) - V_I\cos(\sigma + \alpha)$$

$$R\Omega = V_I\sin(\sigma + \alpha) - V_T\sin\left(\sigma + \theta - \gamma_T\right)$$

[redacted]

The quantities R, σ, θ, and α are defined as:

$$R = R_o + \int \dot{R}\, dt$$

$$\sigma = \sigma_o + \int \dot{\sigma}\, dt = \sigma_o + \int (\Omega - \dot{\theta})dt$$

$$\theta = \theta_o + \int \dot{\theta}\, dt$$

$$\alpha = \alpha_o + \int \dot{\alpha}\, dt$$

In practice, R, σ, and $\dot{\sigma}$ would be available from the radar; however, in the analog solution of the problem these quantities were obtained from actual integrations.

Certain simplifying assumptions were made in this investigation. The angles $(\sigma + \theta)$ and $(\sigma + \alpha)$ were assumed to be small enough such that the cosines and sines of these angles are equal to unity and to the angle in radians, respectively. For these assumptions

$$\dot{R} \approx V_T\left[\cos\ \gamma_T + (\sigma + \theta)\sin\ \gamma_T\right] - V_I$$

$$R\Omega \approx V_I(\sigma + \alpha) - V_T\left[(\sigma + \theta)\cos\ \gamma_T - \sin\ \gamma_T\right]$$

and the guidance equations are

$$\left.\begin{aligned} R + \dot{R}\left(t_G + \tau\right) - V_R\tau &\approx M_{LS} \\ -R\Omega\left(t_G + \tau\right) - V_R\tau(\sigma + \alpha) &\approx M_{NLS} \end{aligned}\right\} \qquad (4)$$

[redacted]

The solution of equations (4) is accomplished by computing continuously the value of $(t_G + \tau)$ necessary for $M_{LS} = 0$ from the first of these equations and for this value of $(t_G + \tau)$ computing the value of M_{NLS} which will exist at $(t_G + \tau)$ seconds subsequent to the instantaneous time from the second of equations (4). The time at which t_G is computed to be zero is the firing point for the interceptor's rockets. The time of flight of the interceptor's rockets is τ, and throughout this investigation is assumed to be 1.5 seconds. The command to the control system is based on the error ϵ_γ which exists at any time in the interceptor's flight path, which for this investigation was approximated by the expression

$$\epsilon_\gamma \approx - \frac{M_{NLS}}{V_I t_G + \left(V_I + V_R\right)\tau} \tag{5}$$

The validity of the foregoing assumptions in the guidance equations were checked by a digital solution on the Bell Telephone Laboratories X-66744 relay computer at the Langley Laboratory where the exact guidance equations were used. This comparison is discussed in a later section.

Discussion of Flight-Path Control System

The block diagram of the overall system is presented in figure 2. Briefly, the computed quantity ϵ_γ is filtered, amplified, and used as the command to a pitch-rate command system. The dynamics of the filter and elevator servo are represented by simple first-order lag networks of the form $\frac{1}{1 + \tau_f D}$ and $\frac{1}{1 + \tau_s D}$, respectively. The transfer function $\frac{1}{1 + \tau_f D}$ is assumed to be representative of a low-pass filter which in practice would be necessary to attenuate the high-frequency radar noise present in the computed command signal ϵ_γ. However, no attempt was made to include noise in the present investigation. The dynamics of the interceptor were obtained from the linearized equations of longitudinal motion. For certain cases, these equations were modified to include specific nonlinearities. All of the equations used in the analysis and the analog schematic diagram are presented in appendix A. The interceptor parameters and other constants used in the analysis are presented in table I. The interceptor stability derivatives and mass parameters were obtained from unpublished data and the results of reference 1.

[redacted]

SCOPE OF INVESTIGATION

The investigation may be conveniently divided into several parts, namely:

(1) Preliminary determination of system gains.

(2) Effects of nonlinear variations of drag, lift, and pitching moment on attack performance.

(3) Effects of changes in forward velocity.

(4) Study of the effect of system gains and other parameters.

(5) Effect of limits on deflection and rate of deflection of the elevator.

(6) Discussion of normal acceleration limiter.

RESULTS AND DISCUSSION

Selection of System Gain Constants and Effects of Various Aerodynamic Parameters on Attack Performance

Prior to the general study an investigation was made to determine values of the gain constants K and K_r for which the attack performance of the interceptor would be reasonably satisfactory as a starting point for the general study. The servo gain constant K_s is taken as unity throughout this paper. Examination of the block diagram (fig. 2) indicates that the forward-loop gain is KK_s and the feedback gain is K_rK_s, and hence the assumption that K_s equals unity imposes no restrictions on the system gain constants or performance. From a theoretical analysis of the open-loop frequency response γ/ϵ_γ and several preliminary runs on the REAC, acceptable values of K and K_r were found to be 3.0 and 0.375, respectively.

For these values of K and K_r tracking runs were computed for $R_o = 60{,}000$ feet, $\gamma_T = \pi$, and $\sigma_o = 7.5^\circ$ and 15° and are presented in figure 3. For these runs the interceptor motions were computed from the linearized equations of longitudinal motions presented in appendix A.

[redacted]

The responses shown in figure 3 include the predicted miss distance normal to the line of sight (M_{NLS}), interceptor normal acceleration (n), elevator deflection (δ_e), and relative change in interceptor forward velocity $\left(u' = \frac{\Delta V}{V_{I_o}}\right)$. For these runs the elevator deflection was limited to $\pm 20^\circ$ and the rate of elevator deflection was limited to $\pm 120^\circ$/sec. The miss distance M_{NLS} was started off-scale on the REAC recorder in order to bring out more clearly the characteristics of M_{NLS} in the vicinity of zero. For all runs presented in this paper, the transient responses are plotted up to the time at which the interceptor's rockets are assumed to be fired ($t_G = 0$). In view of the small angle assumptions made in deriving the guidance equations (eqs. (4)), the quantity $(t_G + \tau)$ is dependent only upon the initial range R_o, target velocity V_T, rocket velocity V_R, rocket time of flight τ, and interceptor forward velocity $V_{I_o}(1 + u')$; and for small values of u', the parameter $(t_G + \tau)$ varies linearly with time. For $\sigma_o = 7.5^\circ$ the change in forward velocity is $0.07V_{I_o}$, the value of M_{NLS} at the assumed time of firing is -30 feet, and the peak normal acceleration is 7.6g. For $\sigma_o = 15^\circ$, the change in forward velocity is $0.14V_{I_o}$, $M_{NLS} = -90$ feet, and the peak acceleration is 7.8g. For both values of σ_o, the maximum perturbation in α was about 0.28 radian, but these transients are not presented.

The miss distance M_{NLS} for neither of these runs is zero at the end of the run, but this condition is not due to the choice of gain constants. These nonzero values of M_{NLS} can be attributed to the decrease in the interceptor's forward velocity during the runs. The interceptor is unable to maintain a condition of steady tracking $(n = 0, \ M_{NLS} = 0)$ as long as the forward velocity varies since, for the type of guidance considered, the interceptor must fly a constant flight path with constant velocity in order for the flight-path error ϵ_γ to be continuously zero. For these runs, u' never attains a constant value and consequently M_{NLS} is not zero at the assumed firing time.

Effect of nonlinear variation of drag and lift with angle of attack and Mach number.- From unpublished wind-tunnel tests made for a model similar to the interceptor discussed in this paper, the variation of the drag coefficient C_D in the vicinity of the interceptor's trim angle of attack ($\alpha_o = 0.033$ radians) and initial Mach number ($M_o = 2.2$) was found

[redacted]

to be well approximated by the expression

$$C_D = 0.014 + \frac{0.024}{M} + \left(\frac{5.92}{M} - \frac{1.58}{M^2}\right)\alpha^2$$

and the variation of C_{L_α} with Mach number in this range was given by

$$C_{L_\alpha} = \frac{5.05}{M} \text{ per radian}$$

If Mach number effects on C_D and C_{L_α} are neglected, these expressions become, for $\alpha_o = 0.033$ radians and $M_o = 2.2$,

$$\left.\begin{aligned} C_D &= 0.027 + 0.156\Delta\alpha + 2.37(\Delta\alpha)^2 \\ C_{L_\alpha} &= 2.29 \text{ per radian} \end{aligned}\right\} \quad (6)$$

The expressions for C_D and C_{L_α}, if only first-order changes in M are considered, become

$$\left.\begin{aligned} C_D &= 0.027 + 0.156\Delta\alpha + 2.37(\Delta\alpha)^2 - \left[0.013 + 0.134\Delta\alpha + 2.03(\Delta\alpha)^2\right]\frac{\Delta M}{M_o} \\ C_{L_\alpha} &= 2.29\left(1 - \frac{\Delta M}{M_o}\right) \end{aligned}\right\} \quad (7)$$

Tracking responses were computed for $K = 3.0$, $K_r = 0.375$, $R_o = 60{,}000$ feet, and $\sigma_o = 7.5^\circ$ and 15° for the cases where equations (6) and (7) were used for C_D and C_{L_α}. The results are presented in figures 4(a) and 4(b). Also shown in these figures is the case for which ΔC_D is assumed to vary linearly with $\Delta\alpha$, that is, $\Delta C_D = 0.156\Delta\alpha$. For $\sigma_o = 7.5^\circ$ (fig. 4(a)), the change in interceptor forward velocity is seen to be $0.07V_{I_o}$ for the linear case, $0.13V_{I_o}$ when ΔC_D varies

nonlinearly with $\Delta\alpha$, and $0.14V_{I_o}$ when ΔC_D varies nonlinearly with $\Delta\alpha$ and ΔM and C_{L_α} varies with Mach number. For the linear case $M_{NLS} = -30$ feet, and for the nonlinear cases $M_{NLS} \approx -50$ feet. As pointed out previously, the nonzero values of M_{NLS} are due to the change in forward velocity. The same general trends are noted for $\sigma_o = 15^\circ$ (fig. 4(b)), but the changes in forward velocity for this value of σ_o are much greater for each drag condition investigated than were encountered for $\sigma_o = 7.5^\circ$. Also, the values of M_{NLS} at the end of the run are larger for this value of σ_o than for $\sigma_o = 7.5^\circ$.

Effect of feedback proportional to change in forward velocity.- A possible means of eliminating, or at least reducing, the value of M_{NLS} at the assumed firing time is to feed back a signal to the elevator servo proportional to the change in forward velocity, such that a positive pitching moment is produced for a decrease in forward velocity. Runs are presented in figures 5(a) and 5(b), for the case where C_D varies nonlinearly with $\Delta\alpha$ and ΔM, for $\sigma_o = 7.5^\circ$ and 15° in which is incorporated a feedback gain of 0.12. For each value of σ_o the predicted value of M_{NLS} is seen to be appreciably reduced. This type of feedback requires a bias error in the flight path in order for the interceptor to fly a constant flight path; but, on the basis of the predicted value of M_{NLS} presented in figure 5, this bias appears to be small. For comparison runs in which the change in forward velocity was assumed to be zero are also shown in these figures. Despite the fact that the velocity changed considerably during these runs, there appears to be no appreciable difference between the cases which included the feedback proportional to u' in which forward velocity was allowed to vary, and the cases which neglected velocity changes. On the basis of these results, the remaining runs presented in this paper were computed with the assumption that velocity changes can be made to have a negligible effect on the attack performance of the interceptor being discussed.

Effect of variations in the pitching moment due to angle of attack.- Recent results of wind-tunnel tests of complete models have often indicated a nonlinear variation of pitching moment with angle of attack. In order to check, at least qualitatively, the effect of a nonlinear pitching moment, runs were made for the assumed pitching variation presented in figure 6(a). This variation of C_m with angle of attack is generally similar to the type of variation obtained from wind-tunnel tests, but it should be pointed out that the range of α for which the pitching moment is nonlinear was arbitrarily selected on the basis of this range of α being in the range likely to be encountered in this particular problem. The results for this variation are presented in figure 6(b) and afford

[redacted]

a comparison between the linear and nonlinear cases. For these runs $K = 3.36$, $K_r = 1.0$, $R_o = 60{,}000$ ft, and $\sigma_o = 7.5^\circ$. The altitude and Mach number of the interceptor and target are the same as before. The most significant effects of the assumed nonlinearity appeared to be reflected in the M_{NLS}, n, and δ_e transients and hence these are the variables presented in figure 6(b). The maximum normal acceleration is about 9g for the nonlinear case as compared to approximately 7g for the linear case. The nonlinear case also shows that there is considerable overshoot in the M_{NLS} transient, and the δ_e motion is rather irregular. It should be noted, however, that this assumed nonlinearity does not prevent the predicted M_{NLS} from being approximately zero at the assumed time of firing. The results obtained for this assumed pitching-moment variation are in agreement with those which would have been intuitively expected. The slope of the pitching-moment curve (fig. 6(a)) is seen to decrease in magnitude as the angle of attack increases, and finally reverses its sign. The general effect of reducing C_{m_α} is to reduce the system spring constant in pitch and hence to increase the static sensitivity between pitching velocity (or normal acceleration) and elevator deflection. This effect is reflected in the larger normal acceleration for the nonlinear case.

General Effect of Control System Parameters and Initial Conditions on Attack Performance

Tracking runs were computed which indicate the general effect on the system performance of variations in the gain constants and other system parameters. The comparisons are presented in the form of REAC runs and in the form of summary plots which indicate the effect of the various quantities on factors such as rise time, response time, and maximum overshoot with respect to the miss distance M_{NLS}, and maximum normal acceleration encountered during the run. In this investigation rise time is defined as the time required for M_{NLS} to initially reach the point of zero miss and response time as the time for M_{NLS} to reach and remain less than 30 feet.

Effect of the tracking loop gain K.- The effect of the gain constant K on the system performance is shown in figure 7 for values of σ_o equal to 7.5° and 15°. The results are presented for $K = 3$, 5, and 9. For these cases the initial range was 60,000 feet and the feedback gain K_r was equal to 0.375. The effect of K is seen to be essentially the same for both values of σ_o. As the gain is increased the system becomes more and more oscillatory and for $K = 9.0$ the M_{NLS}

response is probably unsatisfactory for both values of σ_o. The effects of K, with respect to rise time, response time and overshoot of the M_{NLS} transient, and maximum normal acceleration encountered are summarized in figure 7(c) for $\sigma_o = 7.5^\circ$ and 15°. As K is increased, there is only a slight variation in rise time and peak acceleration, which is due, to a large extent, to the fact that the elevator reaches its maximum deflection of -20° very quickly and remains at that deflection for a time dependent upon K and σ_o. As K is increased, the response time tends first to decrease, and then become large as K is further increased. The response time for $K = 9$ and $\sigma_o = 15^\circ$ is not shown, since for this combination of K and σ_o, M_{NLS} never reaches the condition where it remains less than 30 feet. For both values of σ_o, the overshoot in M_{NLS} increases progressively with increases in K.

Effect of rate feedback gain K_r.- For $K = 3.0$, $\sigma_o = 7.5^\circ$, and $R_o = 60{,}000$ feet, results are presented in figure 8(a) for values of $K_r = 0$, 0.20, 0.375, 0.60, and 1.0. For $K_r = 0$ the responses are seen to be rather oscillatory. As K_r is increased the system becomes more stable, but the overshoot in M_{NLS} is seen to increase with increases in K_r. These effects are due to the fact that, as the interceptor is stabilized, its response to control inputs becomes slower; hence the resultant increase in the M_{NLS} overshoot. A summary of the effects of K_r on the M_{NLS} transient are presented in figure 8(b). Inclusion of the pitch-rate feedback tends to reduce the response time and overshoot of M_{NLS} and, in addition, to eliminate the oscillatory condition which exists for $K_r = 0$; but for values of K_r greater than 0.375, the overshoot is larger than for $K_r = 0$. There is seen to be a relatively negligible effect of K_r on the rise time which, as mentioned previously, is due to the fact that δ_e is at its limit of -20° at the beginning of the run and the rate feedback is ineffective during the early portion of the run.

Effect of initial error in σ.- For $K = 3.0$, $K_r = 0.375$, and $R_o = 60{,}000$ feet, several runs were made to evaluate the ability of the system to score a hit as the initial error in σ is increased. The value of σ actually reflects the altitude difference and the horizontal distance between the interceptor and target; at the beginning of the run the altitude difference is given by the expression $R_o \sin(\sigma_o + \theta_o)$. Results are presented in figure 9 for $\sigma_o = 2^\circ$, 7.5°, 10°, 15°, and 20°. As σ_o is increased, the time which elapses between reaching the correct flight path ($M_{NLS} = 0$) and the firing point becomes less and less, until

[redacted]

for $\sigma_o = 20^o$ the interceptor is unable to reduce M_{NLS} to zero. The maximum allowable initial value of σ_o is a function of the range and the maximum g the airplane can pull. In the present system for $\delta_{e_L} = -20^o$, n_{ss} is approximately 5g.

There is presented in figure 10 a plot of the initial range R_o against the maximum initial σ_o for which the present system could score a hit. This curve was obtained from a simultaneous solution of the equations

$$\left.\begin{aligned} V_I \int_0^{t_G} \cos\left[\gamma(t)\right] dt + \left(V_I + V_R\right)\tau \cos\left[\gamma(t_G)\right] - V_T \cos \gamma_T(t_G + \tau) \\ = R_o \cos(\sigma_o + \theta_o) \\ V_I \int_0^{t_G} \sin\left[\gamma(t)\right] dt + \left(V_I + V_R\right)\tau \sin\left[\gamma(t_G)\right] - V_T \sin \gamma_T(t_G + \tau) \\ = R_o \sin(\sigma_o + \theta_o) \end{aligned}\right\} \quad (8)$$

for the case where $\gamma_T = \pi$. Equations (8) relate the horizontal and vertical distances traveled by the interceptor, rockets, and target to the horizontal and vertical distances which exist between the interceptor and target at $t = 0$. If these equations were satisfied, a hit would be obtained. The function $\gamma(t)$ was calculated from the longitudinal equations of motion for a step input on $\delta_e = -20^o$, which is taken as the maximum value of δ_e throughout this paper. Also presented in figure 10 is the variation of R_o with σ_o which was calculated on the assumption that $\gamma(t) = \gamma(o) + \dot{\gamma}t$. The value of $\dot{\gamma}$ used in this expression is the steady-state $\dot{\gamma}$ due to an elevator deflection of -20^o, and it was assumed that the airframe attained this output immediately upon application of control. The results obtained for this simplified approach to the problem are seen to be substantially the same as those obtained using the more exact approach. The curve indicates that for $R_o = 60{,}000$ feet the largest σ_o which can be used is approximately 22^o. As a check, runs were made for a large value of K (in order to keep $\delta_e = (\delta e)_L$ for the entire run) and the results indicated that $\sigma_o = 20^o$ was about the largest value which could be tolerated.

[redacted]

In order to obtain a hit for R_o = 60,000 feet and $\sigma_o \approx 22^\circ$, the required time of flight of the interceptor from its initial position to the assumed firing point is seen from figure 10 to be 16.8 seconds. This explains the difference between the maximum allowable σ_o indicated by figure 10 and the value obtained from the REAC results. For the REAC runs, the simplifications made in the guidance equations eliminated the dependence of $(t_G + \tau)$ on σ_o; and for the initial range R_o = 60,000 feet, t_G is equal to 14.8 seconds. Actually, t_G for the REAC runs was slightly less than 14.8 seconds, since R_o was closer to 59,000 feet due to voltage limitations on the REAC. A check was also made for R_o = 30,000 feet and the result also agreed well with the curve of figure 10.

Effect of filter time constant τ_f.- The effect of τ_f is illustrated in figures 11(a) and 11(b) for τ_f = 0, 0.30, 0.60, and 1.2 seconds. For these runs K = 3.0, K_r = 0.375, $\sigma_o = 2^\circ$ and 7.5°, and R_o = 60,000 feet. As τ_f is increased from 0 to 1.2 seconds, the initial response in M_{NLS} is seen to become progressively slower, which is due to the increased lag between the initial command ϵ_γ and the response of the elevator motion. Also, there is seen to be an appreciable overshoot in the M_{NLS} response for τ_f = 1.2 seconds, which is also due to the increased lag between ϵ_γ and the elevator motion. The effects of τ_f on the M_{NLS} are summarized in figure 11(c) for $\sigma_o = 2^\circ$ and 7.5°.

The values of σ_o chosen to illustrate the effect of τ_f have no special significance, but were used only on the basis that the results obtained for these values of σ_o were typical of the results obtained for all values of σ_o up to the maximum allowable value for R_o = 60,000 feet. The same statement may be made concerning the values of σ_o used in the subsequent sections.

Effect of servo time constant τ_s.- The effect of the servo time constant τ_s is demonstrated in figure 12 for τ_s = 0.03, 0.10, 0.20, and 0.30 second. The cases presented are for K = 3.0, K_r = 0.375, $\sigma_o = 2^\circ$, and R_o = 60,000 feet. As τ_s is increased from 0.03 second to 0.30 second, the most important effect is that the overshoot in the M_{NLS} response is seen to become larger, but at the assumed firing point the miss distance is zero in either case. The effects of τ_s on the M_{NLS} response are summarized in figure 12(b).

[redacted]

Effect of control-surface limitations.- The effects of limitations on the rate of control-surface deflection and the magnitude of the surface deflection were investigated briefly for $K = 3.0$, $K_r = 0.375$, and $R_o = 60{,}000$ feet. All of the results presented in this paper up to this point were obtained for the condition where $\dot{\delta}_e$ was limited to $\pm 120^\circ$/sec and δ_e to $\pm 20^\circ$. The effect of reducing the maximum value of $\dot{\delta}_e$ to $\pm 60^\circ$/sec and $\pm 30^\circ$/sec for this tracking run may be seen from figure 13(a). For these runs $\sigma_o = 10^\circ$. The limiting control deflection was kept at $\pm 20^\circ$. The effect on this run of reducing $(\dot{\delta}_e)_L$ was to reduce slightly the peak normal acceleration as $(\dot{\delta}_e)_L$ is reduced from $\pm 120^\circ$/sec to $\pm 30^\circ$/sec. This reduction in g causes a slight increase in the rise and response time of M_{NLS}, but it may be concluded that, at least for this case, the effects of limitations on the rate of control deflection were small. However, for cases where higher values of K would be required (for example, a maneuvering target) the effects of rate limitation would probably be much more important and should be investigated thoroughly. The effects of limiting $\dot{\delta}_e$ on the M_{NLS} responses are summarized in figure 13(b).

Several runs were made for the case of $(\dot{\delta}_e)_L = \pm 120^\circ$/sec and $(\delta_e)_L$ reduced from $\pm 20^\circ$ to $\pm 10^\circ$; the results are presented in figure 14. For these cases σ_o is equal to 5°. The general effect of reducing the control deflection limits from 20° to 10° is to reduce the peak normal acceleration of the interceptor, and hence the rise and response time of the M_{NLS} response. The maximum σ_o for which M_{NLS} can be reduced to zero is directly dependent on the limit imposed on δ_e.

Effect on tracking of limiting the command $\dot{\theta}_i$.- Since the result obtained from filtering and amplifying the error signal ϵ_γ is used as the command to a pitch-rate command system, this command should be limited if it is desired to limit the interceptor's normal acceleration from aerodynamic, pilot comfort, structural, or other considerations. The normal acceleration response to $\dot{\theta}_i$ is given by

$$n = \left(\frac{n}{\dot{\theta}_i}\right)\dot{\theta}_i = \left(\frac{n}{\dot{\theta}}\right)\left(\frac{\dot{\theta}}{\dot{\theta}_i}\right)\dot{\theta}_i \qquad (9)$$

[redacted]

Hence the steady-state normal acceleration can be limited to any desired value by limiting the input command $\dot{\theta}_i$. For the interceptor being considered

$$\left(\frac{\dot{\theta}}{\dot{\theta}_i}\right)_{ss} = \frac{K_s}{\left(\delta_e/\dot{\theta}\right)_{ss} + K_r K_s} = \frac{1}{4.85 + K_r}$$

and, in general,

$$\left(\frac{n}{\dot{\theta}}\right)_{ss} = \frac{V_I}{g}$$

Therefore,

$$(\theta_i)_L = (n)_L(4.85 + K_r)\frac{g}{V_I} \tag{10}$$

If $\dot{\theta}_i$ is limited by this expression, it should be pointed out that only the steady-state n is being limited by use of this expression. The effectiveness of limiting the output transient acceleration by this method depends primarily on the response characteristics of $(n/\dot{\theta}_i)$. If the system gains are chosen to give a fast response of n to $\dot{\theta}_i$ with little or no overshoot, this means of limiting n should be satisfactory. The results presented in figure 15 afford a comparison of the cases for which there is no g-limiter and for the case where g is limited by equation (10). For these cases $K = 3.0$, $K_r = 0.375$, $R_o = 60{,}000$ feet, $\sigma_o = 15^\circ$ and $(n)_L = 5g$. The airframe steady-state normal-acceleration response to the limiting value of δ_e is approximately $4.9g$; hence, the unlimited g case and the case of $(n)_L = 5g$ should oscillate about the same value when $\delta_e = (\delta_e)_L$. As can be seen, the peak n for the unlimited case is roughly $8g$. When $(\theta_i)_L$ is limited by equation (10), the peak g response is reduced roughly to $6.5g$. The rise time of M_{NLS}

[redacted]

is seen to increase slightly when $\dot{\theta}_i$ is limited, but the response time is less than that for the unlimited case.

Digital check on validity of simplified guidance equations.- In order to check the validity of the small-angle assumptions made in the guidance equations (see previous section entitled "Derivation of Guidance Equations"), a solution, using the exact guidance of kinematic equations, was obtained from the Bell Computer for comparison with the REAC tracking solutions which utilized the simplified equations. This comparison is presented in figure 16 for the case of $\sigma_o = 7.5^\circ$, $R_o = 60{,}000$ feet, $K = 3.0$, and $K_r = 0.375$, and the agreement is seen to be excellent.

CONCLUSIONS

The following conclusions were reached from a theoretical investigation of the longitudinal tracking behavior of an automatically controlled interceptor against a nonmaneuvering target:

1. The control system considered in this investigation (i.e., command on rate of pitch proportional to longitudinal tracking error) was found to give acceptable control of the interceptor's flight path during attack runs against a nonmaneuvering target.

2. The inclusion of a nonlinear variation of drag and lift with angle of attack and Mach number resulted in relatively large variations in the interceptor forward velocity during the attack runs.

3. The changes in forward velocity computed for the runs in this investigation, although rather large, had a relatively small effect on the overall responses when a signal proportional to the change in forward velocity was fed back to the elevator servo.

4. Consideration of a nonlinear variation of pitching moment with angle of attack which tended toward static instability at high angles of attack indicated that its primary effect was to increase the magnitudes of the interceptor's motions during the tracking runs.

5. The general effect of increasing the tracking gain K was to destabilize the tracking loop.

6. Increases in the rate-feedback gain K_r tended to stabilize the interceptor's longitudinal short-period oscillation, but had a destabilizing effect on the tracking loop.

[redacted]

7. The maximum initial angularity between the interceptor's flight path and radar line of sight for which a hit can be obtained can be well approximated from the initial range and normal acceleration capabilities of the interceptor.

8. Increases in either the filter time constant τ_f or the servo time constant τ_s had an adverse effect on the attack performance because of the increased lag between the input command and the elevator motions.

9. The effects of limitations on the rate of control deflection did not appear to be large in this investigation for the limiting rates considered.

10. The general effect of limitations on the magnitude of the control deflection was to slow down the interceptor's responses, and hence the maximum initial tracking error which can be tolerated decreases as the limits on elevator deflection are reduced.

11. Limiting of the interceptor normal acceleration was achieved by limiting the input command on pitching velocity, which effectively limits the interceptor's steady-state normal acceleration.

Langley Aeronautical Laboratory,
National Advisory Committee for Aeronautics,
Langley Field, Va., October 22, 1954.

[redacted]

APPENDIX A

EQUATIONS USED IN ANALOG OF TRACKING PROBLEM AND ANALOG SCHEMATIC DIAGRAMS

All of the equations used in this investigation are presented in this appendix. The equations are presented in both symbolic and numerical form. It will be noted that certain of the equations presented in numerical form have been multiplied by constants. This was done in order to adjust the REAC voltages to satisfactory levels in the analog procedure.

Linearized airframe equations ($\gamma_{I_o} = 0$):

$$\left.\begin{aligned}
\ddot{\theta} &= C_{m_q} \frac{\bar{c}}{2V_{I_o}} \frac{qS\bar{c}}{I_Y} \dot{\theta} + C_{m_{\dot{\alpha}}} \frac{\bar{c}}{2V_{I_o}} \frac{qS\bar{c}}{I_Y} \dot{\alpha} + C_{m_\alpha} \frac{qS\bar{c}}{I_Y} \alpha + \\
&\quad C_{m_u}{}' \frac{qS\bar{c}}{I_Y} u' + C_{m_{\delta_e}}{}' \frac{qS\bar{c}}{I_Y} \delta_e' \\
\dot{\alpha} &= \dot{\theta} - C_{L_\alpha} \frac{qS}{mV_{I_o}} \alpha - 2C_L \frac{qS}{mV_{I_o}} u' - C_{L_{\delta_e}}{}' \frac{qS}{mV_{I_o}} \delta_e' \\
\dot{u}' &= -2C_D \frac{qS}{mV_{I_o}} u' - C_L \frac{qS}{mV_{I_o}} \theta - C_{D_\alpha} \frac{qS}{mV_{I_o}} \alpha + C_L \frac{qS}{mV_{I_o}} \alpha
\end{aligned}\right\} \quad (A1)$$

[redacted]

It will be noted that $C_{m_{\delta_e}}'$, $C_{L_{\delta_e}}'$, and δ_e' appear in these equations rather than $C_{m_{\delta_e}}$, $C_{L_{\delta_e}}$, and δ_e. The relations exist that

$$\delta_e' = -\delta_e$$

$$C_{m_{\delta_e}}' = -C_{m_{\delta_e}}$$

$$C_{L_{\delta_e}}' = -C_{L_{\delta_e}}$$

This convention is adopted in order that the true physical phase relationships of the pitch-rate command loop be obtained for positive gain constants.

Control Equations:

$$\left.\begin{aligned} \dot{\epsilon}_f &= \frac{\epsilon_\gamma}{\tau_f} - \frac{\epsilon_f}{\tau_f} \\ \dot{\theta}_i &= K\epsilon_f \\ \dot{\delta}_e' &= K_s\left(\frac{\dot{\theta}_i}{\tau_s} - \frac{K_r\dot{\theta}}{\tau_s}\right) - \frac{\delta_e'}{\tau_s} \end{aligned}\right\} \qquad \text{(A2)}$$

[redacted]

Kinematic equations (simplified, $\gamma_T = \pi$):

$$t_G + \tau = \frac{V_R\tau - R}{\dot{R}}$$

$$\dot{R} = -V_T - V_I$$

$$R\Omega = V_I(\sigma + \alpha) + V_T(\sigma + \theta)$$

$$M_{NLS} = -R\Omega(t_G + \tau) - V_R\tau(\sigma + \alpha)$$

$$\epsilon_\gamma = -\frac{M_{NLS}}{V_I(t_G + \tau) + V_R\tau}$$

$$V_I = V_{I_o} + V_{I_o}u' \qquad \text{(A3)}$$

$$R = R_o + \int \dot{R}\, dt$$

$$\alpha = \alpha_o + \int \dot{\alpha}\, dt$$

$$\theta = \theta_o + \int \dot{\theta}\, dt$$

$$\sigma = \sigma_o + \int (\Omega - \dot{\theta})dt$$

$$\Omega = \frac{R\Omega}{R}$$

[redacted]

For the parameters presented in table I, the preceding equations take the following form:

Airframe equations:

$$\ddot{\theta} = -0.1845\dot{\theta} - 0.01819\dot{\alpha} - 10.382\alpha + 5.469\delta_e'$$

$$\dot{\alpha} = \dot{\theta} - 0.4565\alpha - 0.0303u' + 0.0329\delta_e'$$

$$-20\dot{u}' = 0.215u' + 0.303\theta + 0.579\alpha - 0.303\alpha$$

Control equations:

$$2\dot{\epsilon}_f = 3.333\epsilon_\gamma - 3.333\epsilon_f$$

$$\dot{\theta}_i = K\epsilon_f$$

$$0.05\dot{\delta}_e' = 1.667\dot{\theta}_i - 1.667K_r\dot{\theta} - 1.667\delta_e'$$

Kinematic equations:

$$t_G + \tau = \frac{3000 - R}{\dot{R}}$$

$$12\dot{R} = -16,320 - 12V_I$$

$$20R\Omega = 42,800(\sigma + \alpha) + 27,200(\sigma + \theta)$$

$$-4M_{NLS} = 4R\Omega(t_G + \tau) + 12,000(\sigma + \alpha)$$

$$-2\epsilon_\gamma = \frac{-2M_{NLS}}{-V_I(t_G + \tau) - 3000}$$

[redacted]

$$-20V_I = -42,800 - 42,800u'$$

$$-R = -60,000 - \int \dot{R}\, dt$$

$$-2\alpha = -0.066 - 2\int \dot{\alpha}\, dt$$

$$-\theta = -0.033 - \int \dot{\theta}\, dt$$

$$\sigma = \sigma_o + \int (\Omega - \dot{\theta})dt$$

$$-10\Omega = \frac{-10R\Omega}{R}$$

The α and θ appearing in equations (A3) are total α and θ, whereas the α and θ in equations (A1) are perturbations away from the trimmed condition. The problem was slowed down such that 2 seconds of machine time was equivalent to 1 second of problem time. The scale factors used were: 100 volts = 100 seconds, 100 volts = 1 radian, and 100 volts = 60,000 feet.

In figures 17(a), 17(b), and 17(c) are presented the analog schematics of equations (A1), (A2), and (A3), respectively.

[redacted]

REFERENCE

1. Margolis, Kenneth, and Bobbitt, Percy J.: Theoretical Calculations of the Stability Derivatives at Supersonic Speeds for a High-Speed Airplane Configuration. NACA RM L53G17, 1953.

[redacted]

TABLE I

STABILITY DERIVATIVES AND MASS CHARACTERISTICS

OF INTERCEPTOR AND OTHER CONSTANTS USED

IN INVESTIGATION

Altitude, ft	50,000
ρ, slugs/cu ft	0.0003622
V_{I_o}, ft/sec	2,140(M = 2.2)
m, slugs	776.4
I_Y, slugs-ft^2	2.68 x 10^5
q, lb/sq ft	826
$\bar{c}$, ft	15
S, sq ft	401
C_{m_q}, per radian	-2.84
C_{m_α}, per radian	-0.56
$C_{m_{\dot{\alpha}}}$, per radian	-0.28
C_{m_u}', per radian	0.00
C_{L_α}, per radian	2.29
C_{D_α}, per radian	0.156
C_D	0.027
C_L	0.076
$C_{m_{\delta_e}}$, per radian	-0.295
$C_{L_{\delta_e}}$, per radian	0.165
V_R, ft/sec	2,000
V_T, ft/sec	1,360
τ_s, sec	0.03
τ_f, sec	0.60
τ, sec	1.5
R_o, ft	60,000
θ_o, radians	0.033
α_o, radians	0.033

[redacted]

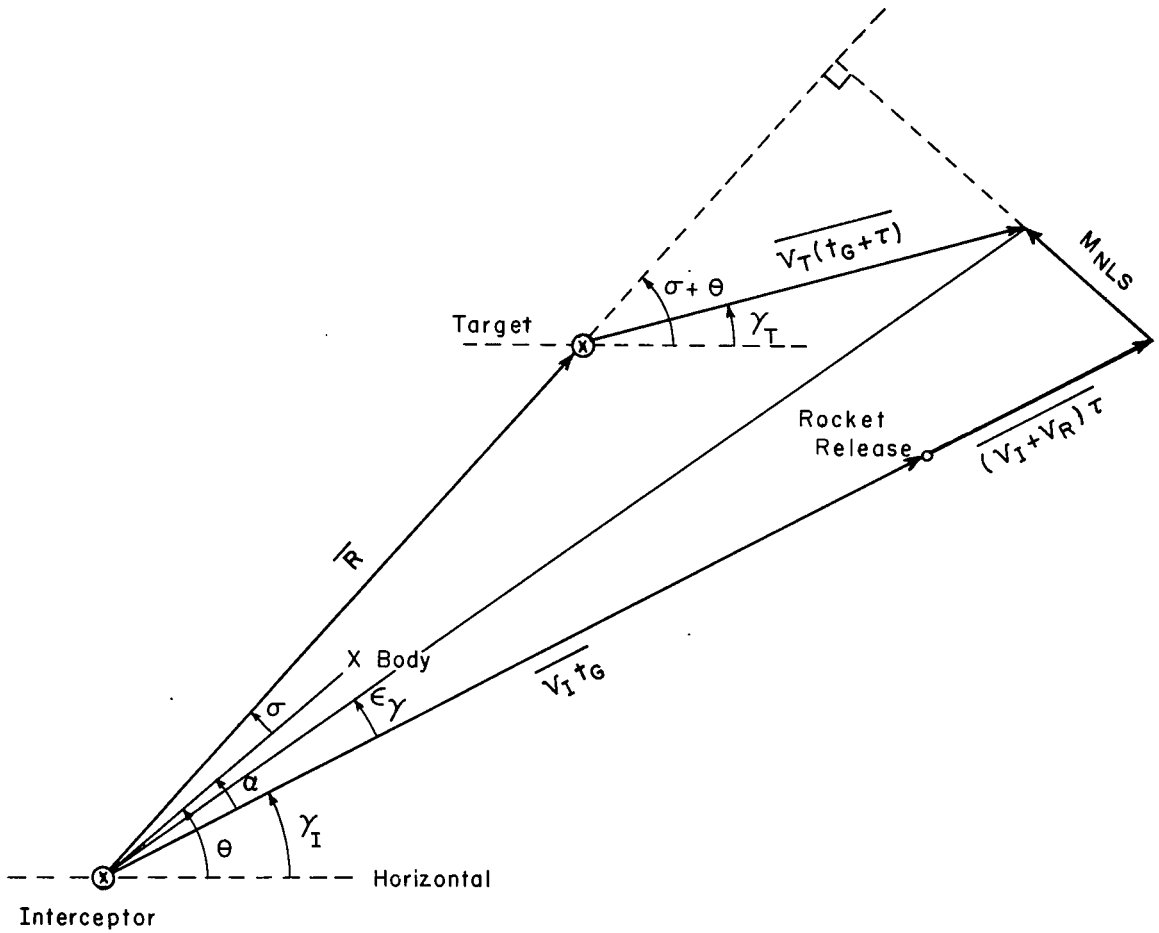

Figure 1.- Geometry of lead collision navigation used in present investigation for $M_{LS} = 0$.

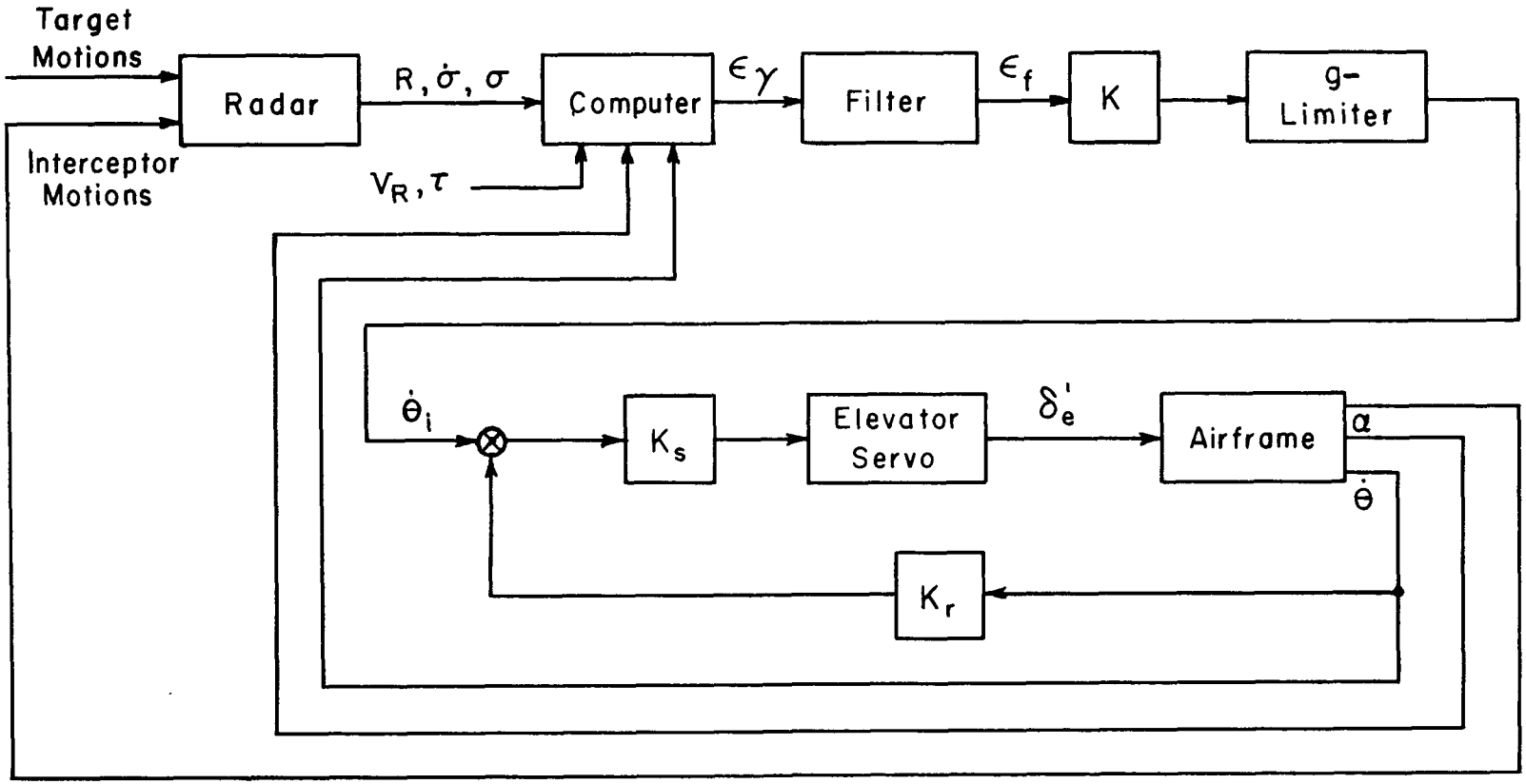

Figure 2.- Block diagram of the longitudinal tracking system used in present investigation.

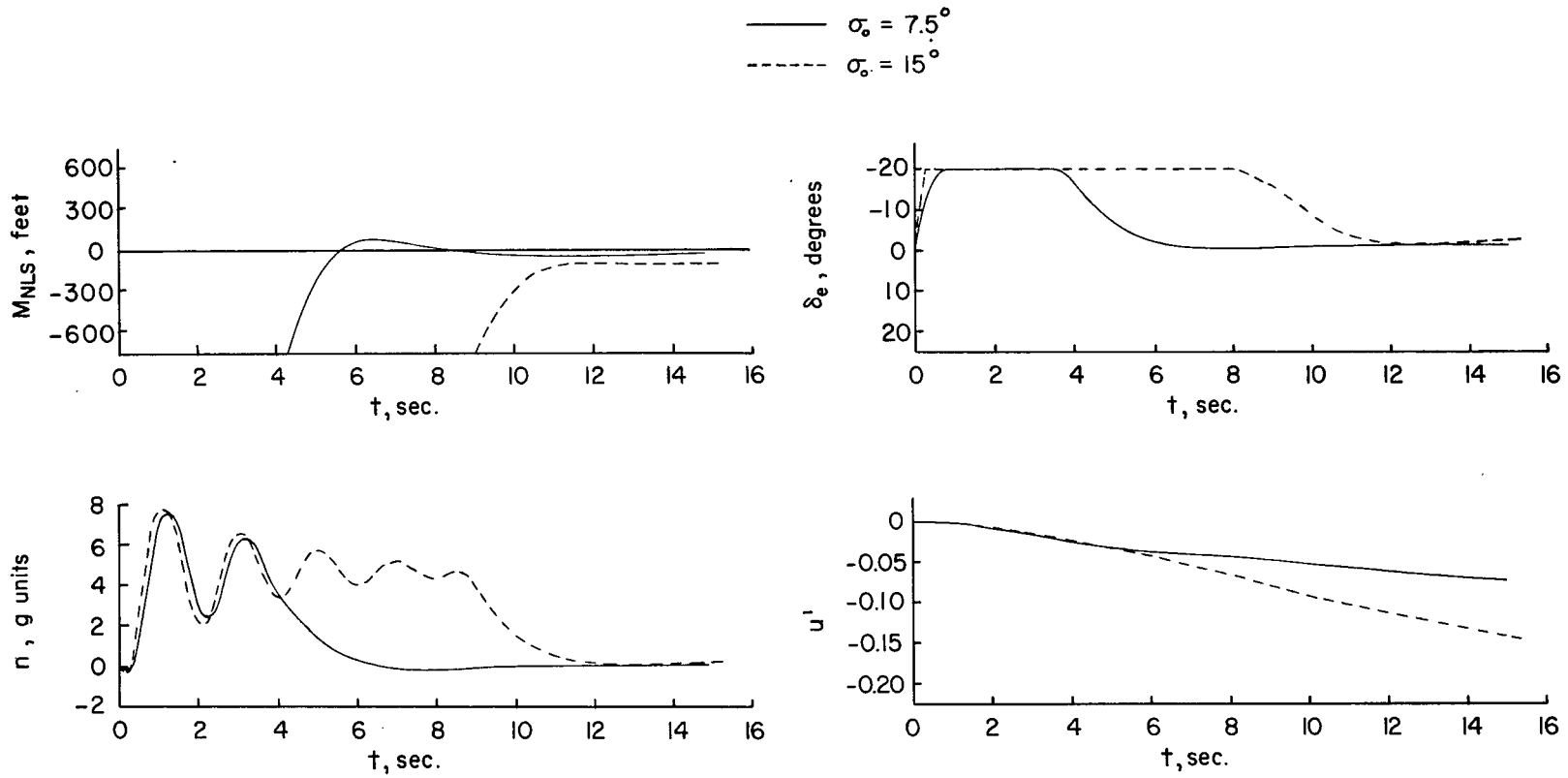

Figure 3.- Interceptor and kinematic time histories for K = 3.0 and K_r = 0.375.

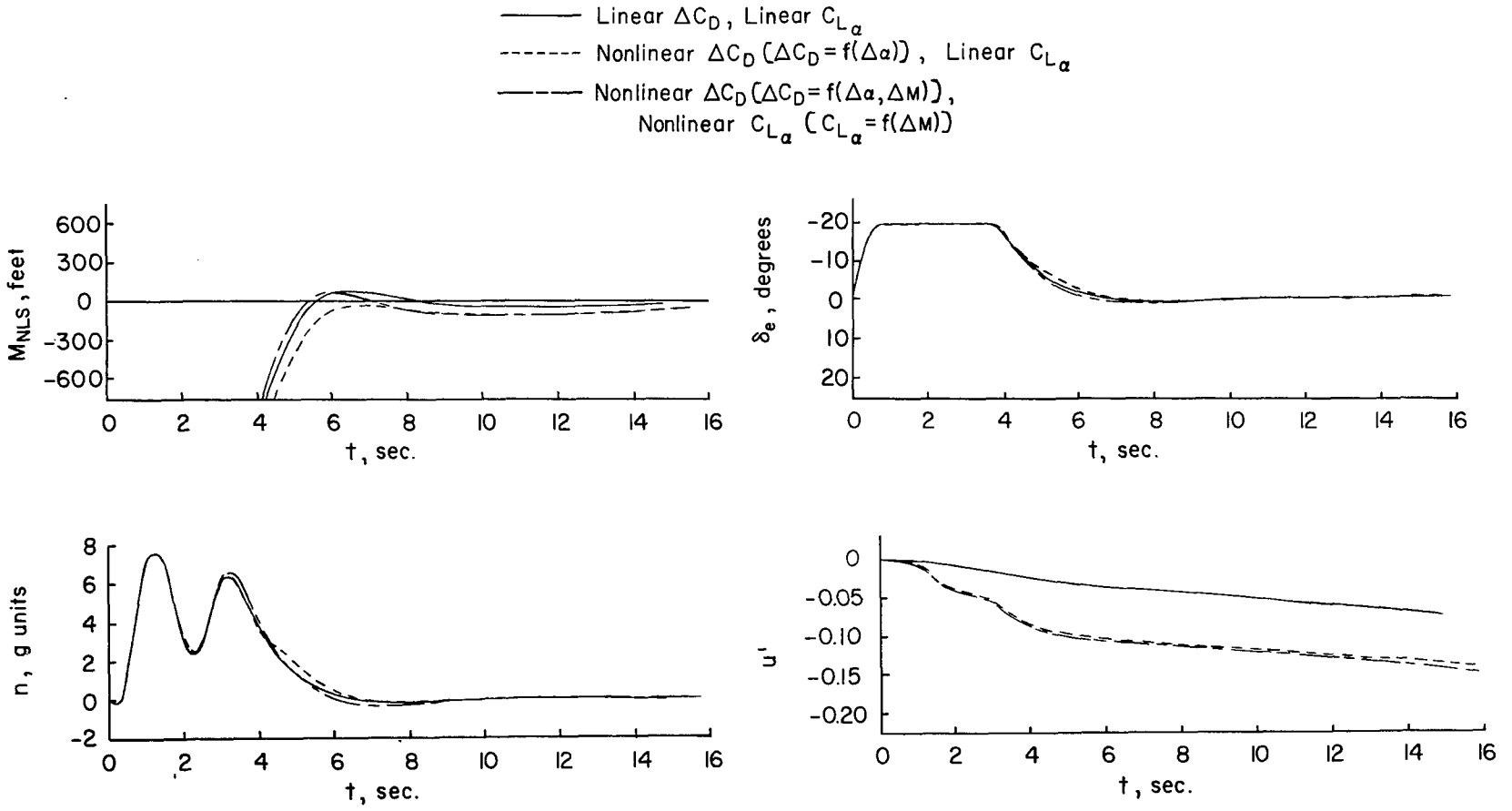

(a) $\sigma_o = 7.5^o$.

Figure 4.- Effect of nonlinear drag and lift on interceptor attack performance. $K = 3.0$; $K_r = 0.375$; $R_o = 60{,}000$ feet.

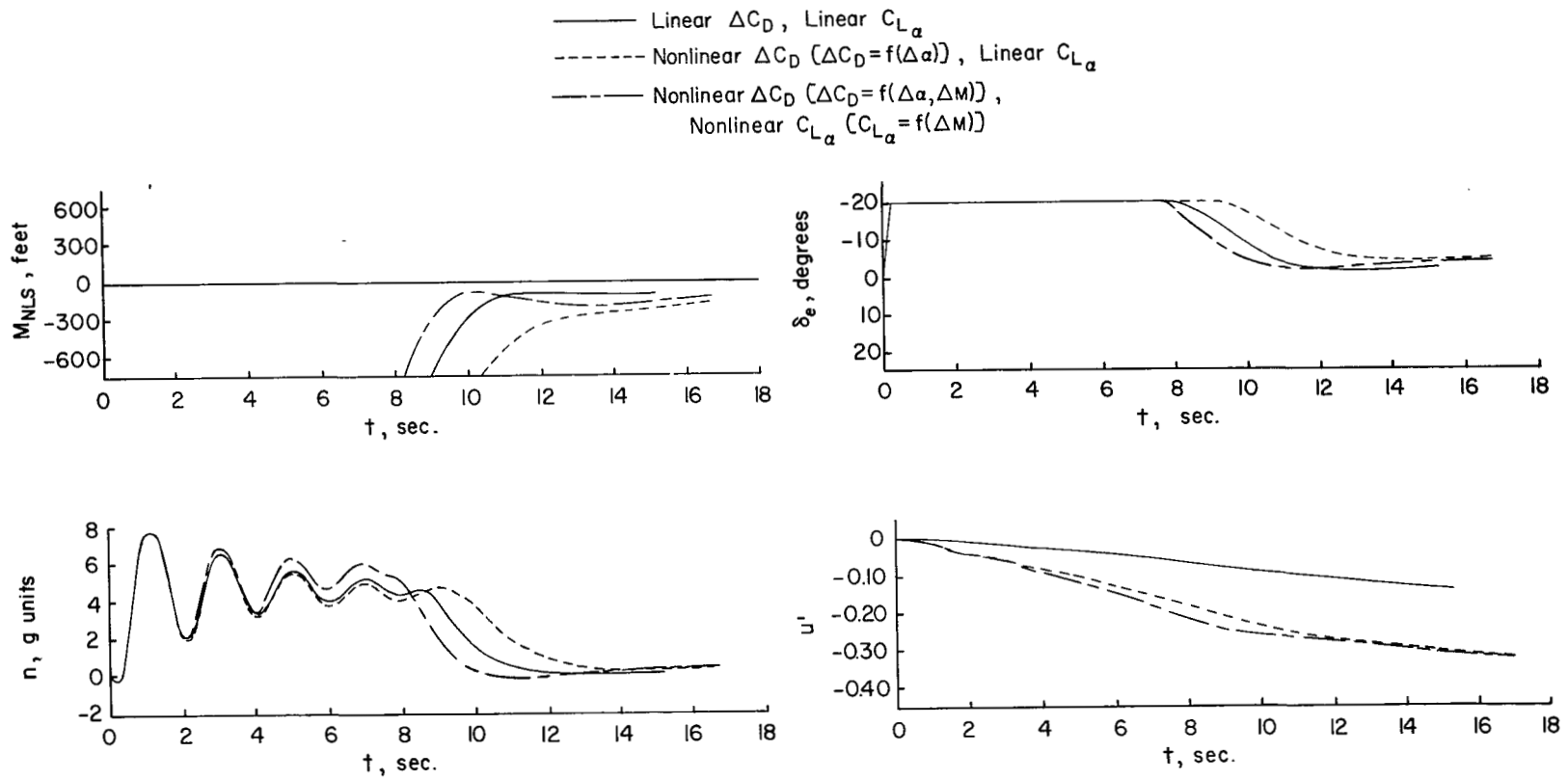

(b) $\sigma_o = 15°$.

Figure 4.- Concluded.

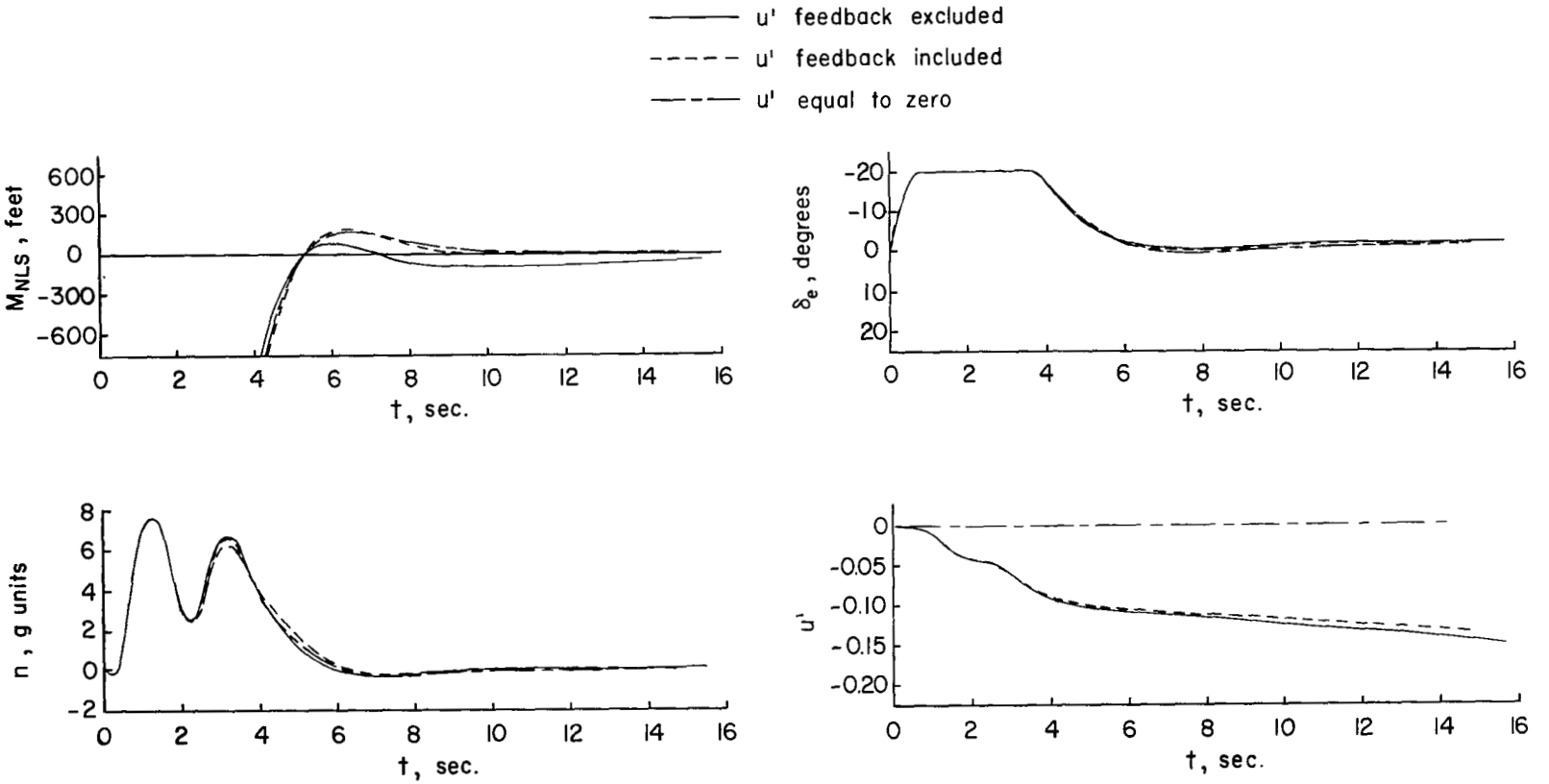

(a) $\sigma_o = 7.5^\circ$.

Figure 5.- Effect of feedback proportional to change in interceptor velocity on interceptor attack performance. $K = 3.0$; $K_r = 0.375$; $R_o = 60{,}000$ feet.

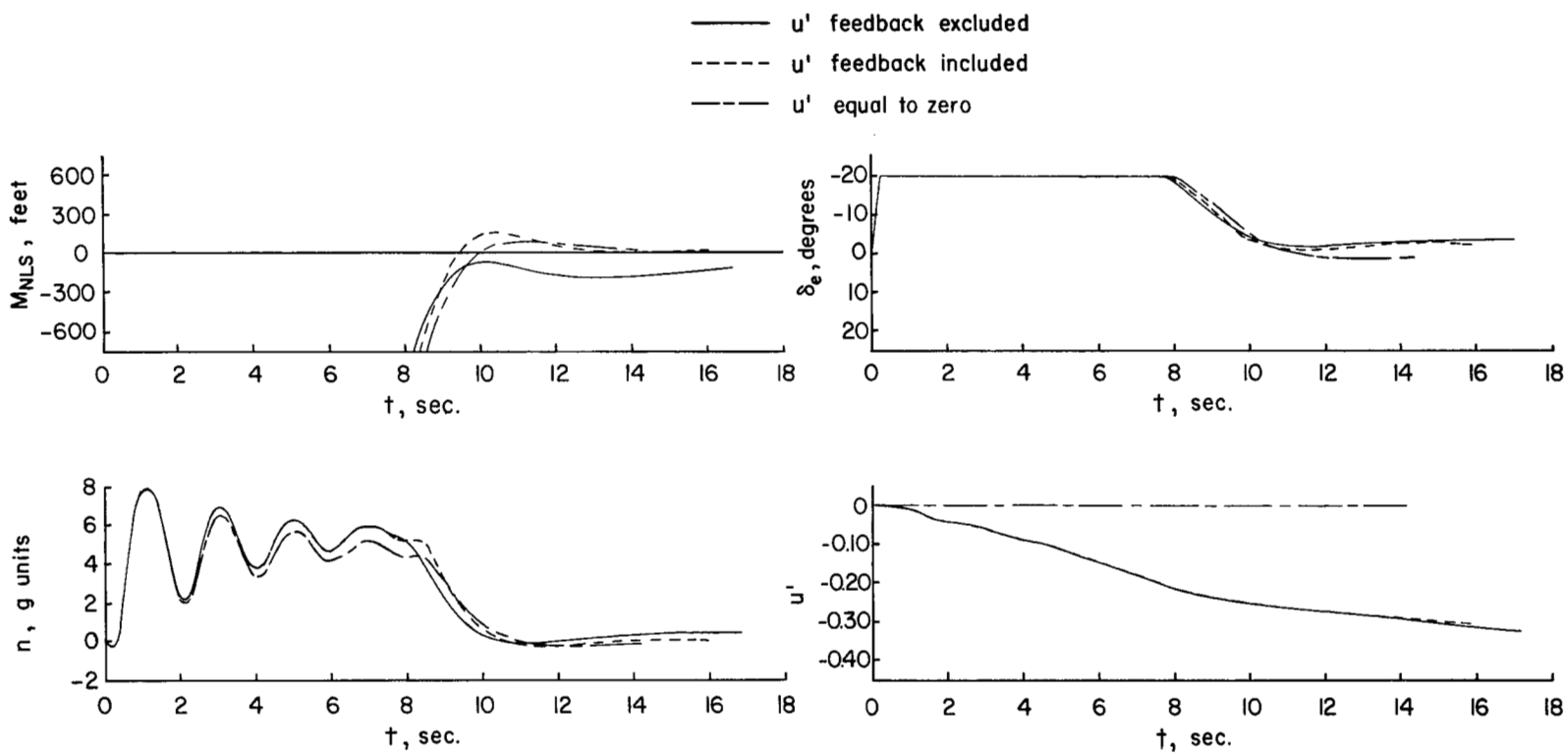

(b) $\sigma_o = 15^\circ$.

Figure 5.- Concluded.

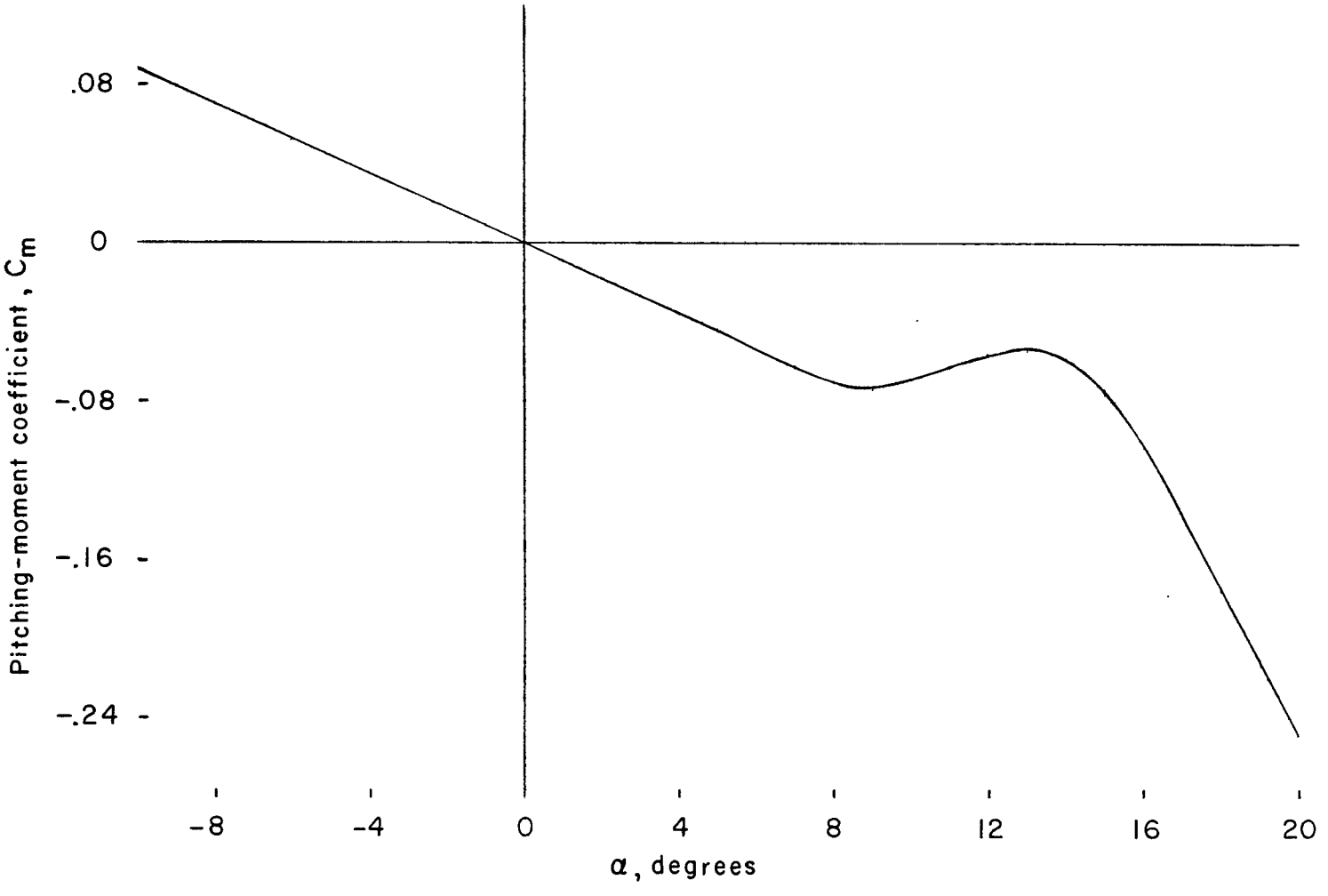

(a) Assumed variation of C_m with α.

Figure 6.- Effect of nonlinear pitching-moment coefficient with angle of attack on interceptor attack performance.

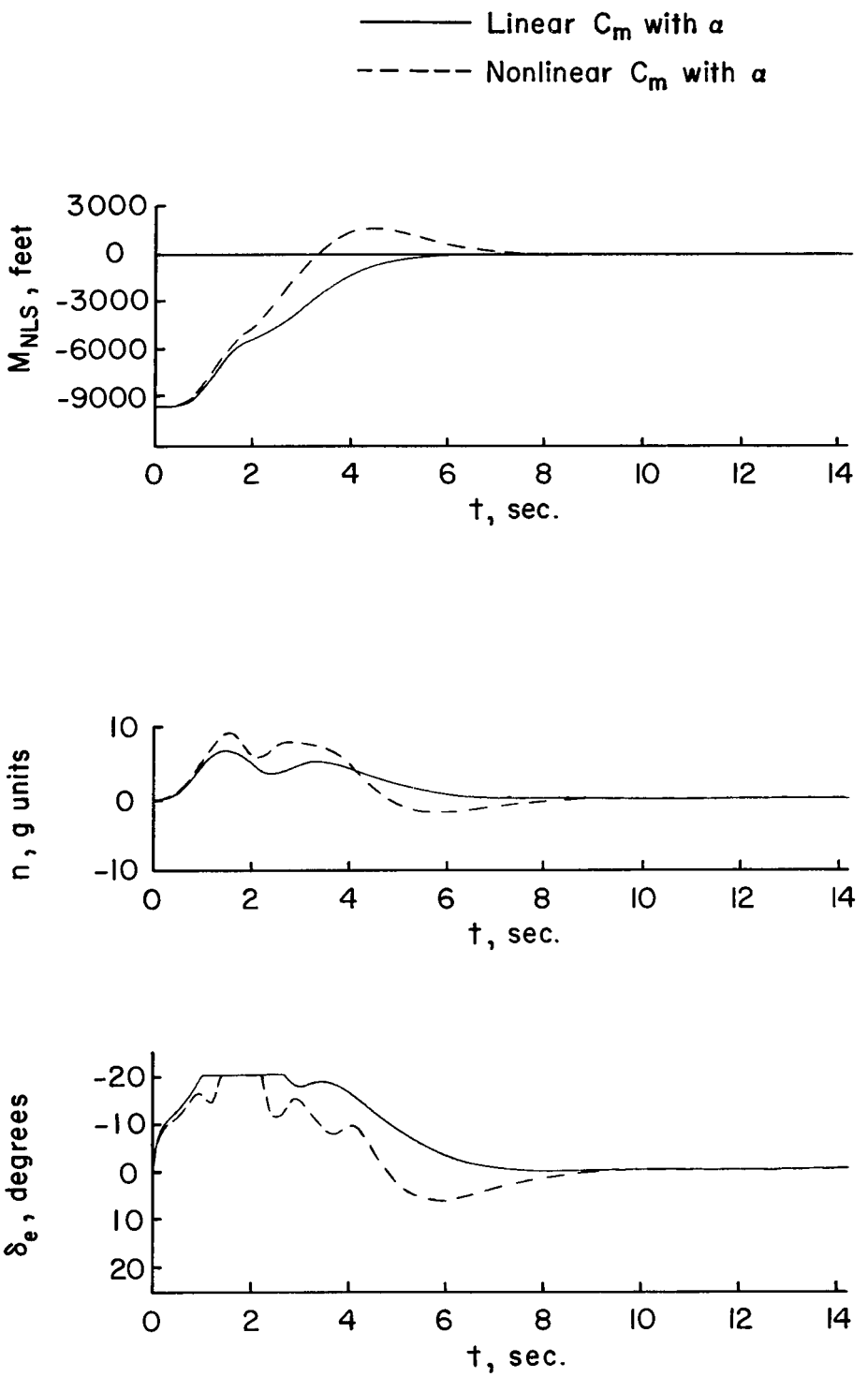

(b) $\sigma_o = 7.5°$.

Figure 6.- Concluded.

[redacted]

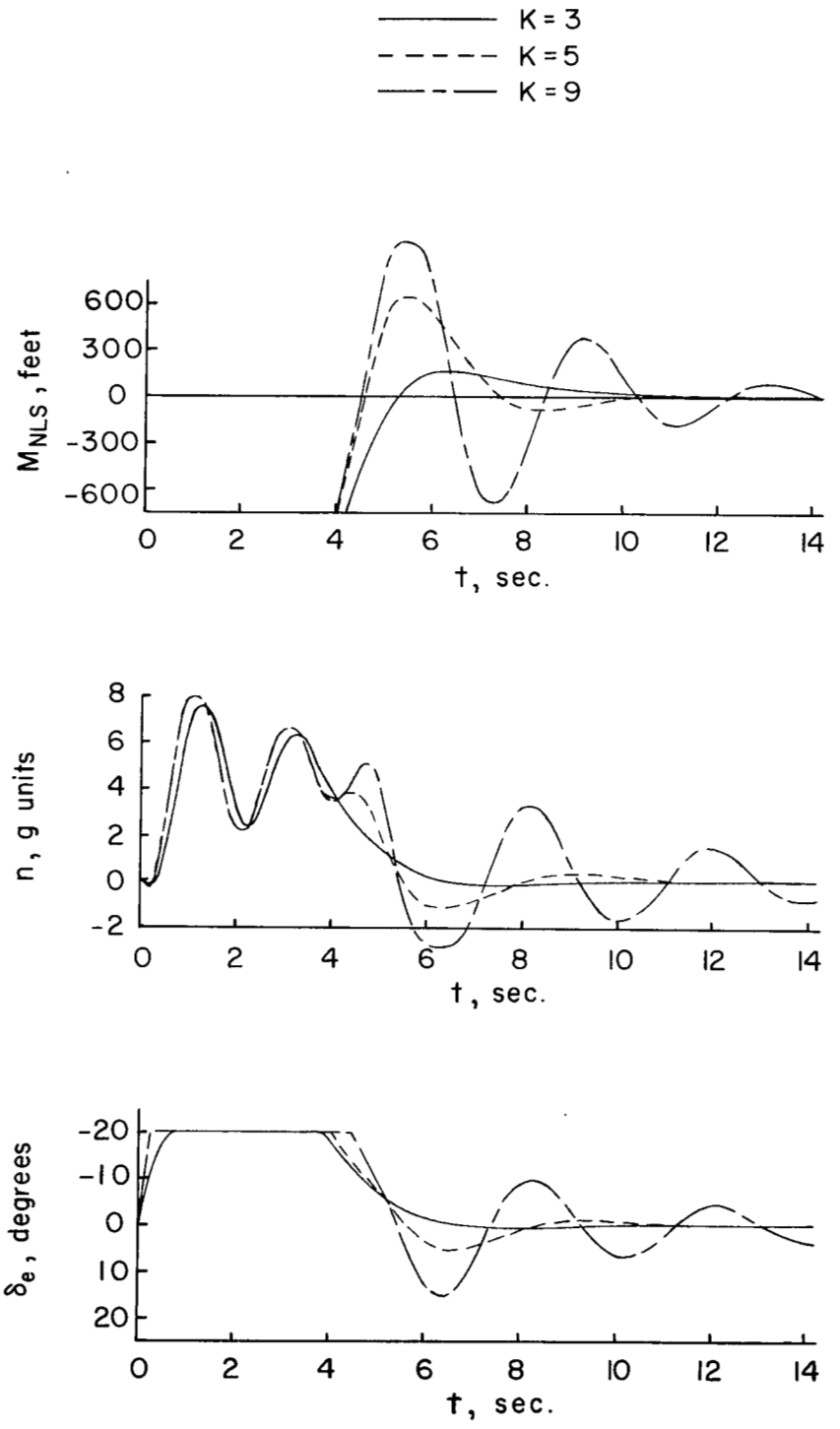

(a) $\sigma_o = 7.5^o$.

Figure 7.- Effect of tracking loop gain K on interceptor attack performance. $K_r = 0.375$; $R_o = 60{,}000$ feet.

[redacted]

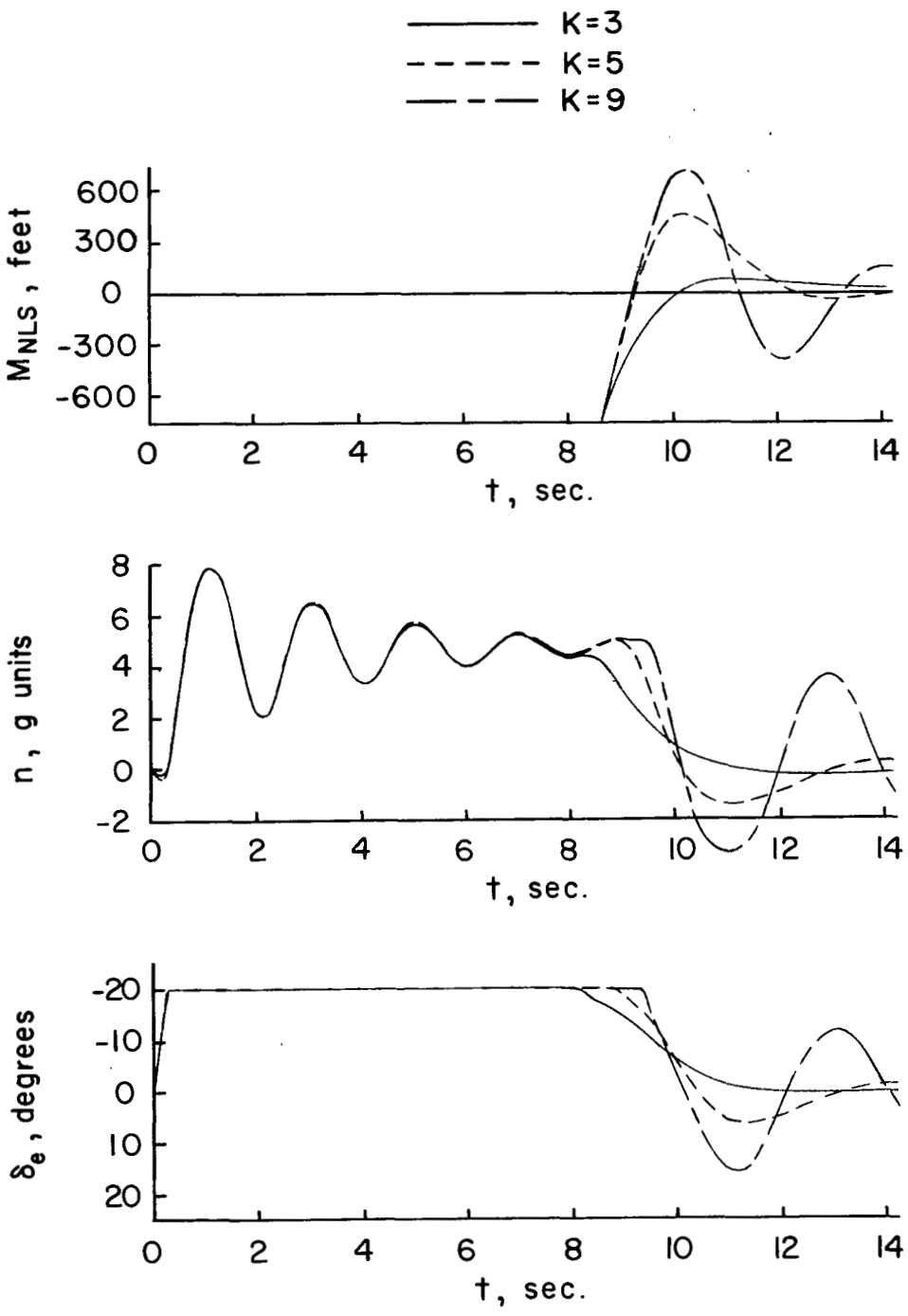

(b) $\sigma_o = 15^\circ$.

Figure 7.- Continued.

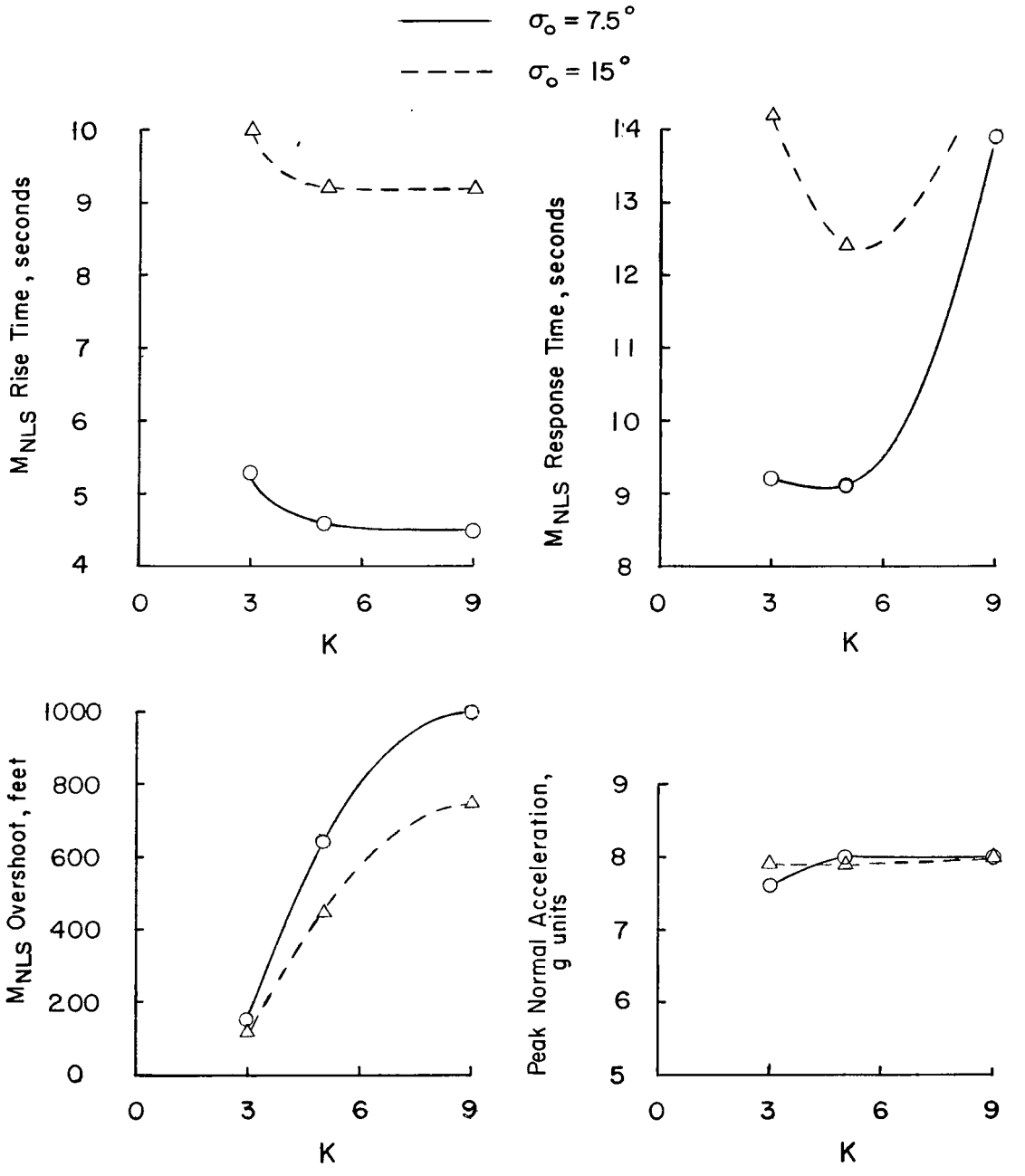

(c) Summary plots.

Figure 7.- Concluded.

[redacted]

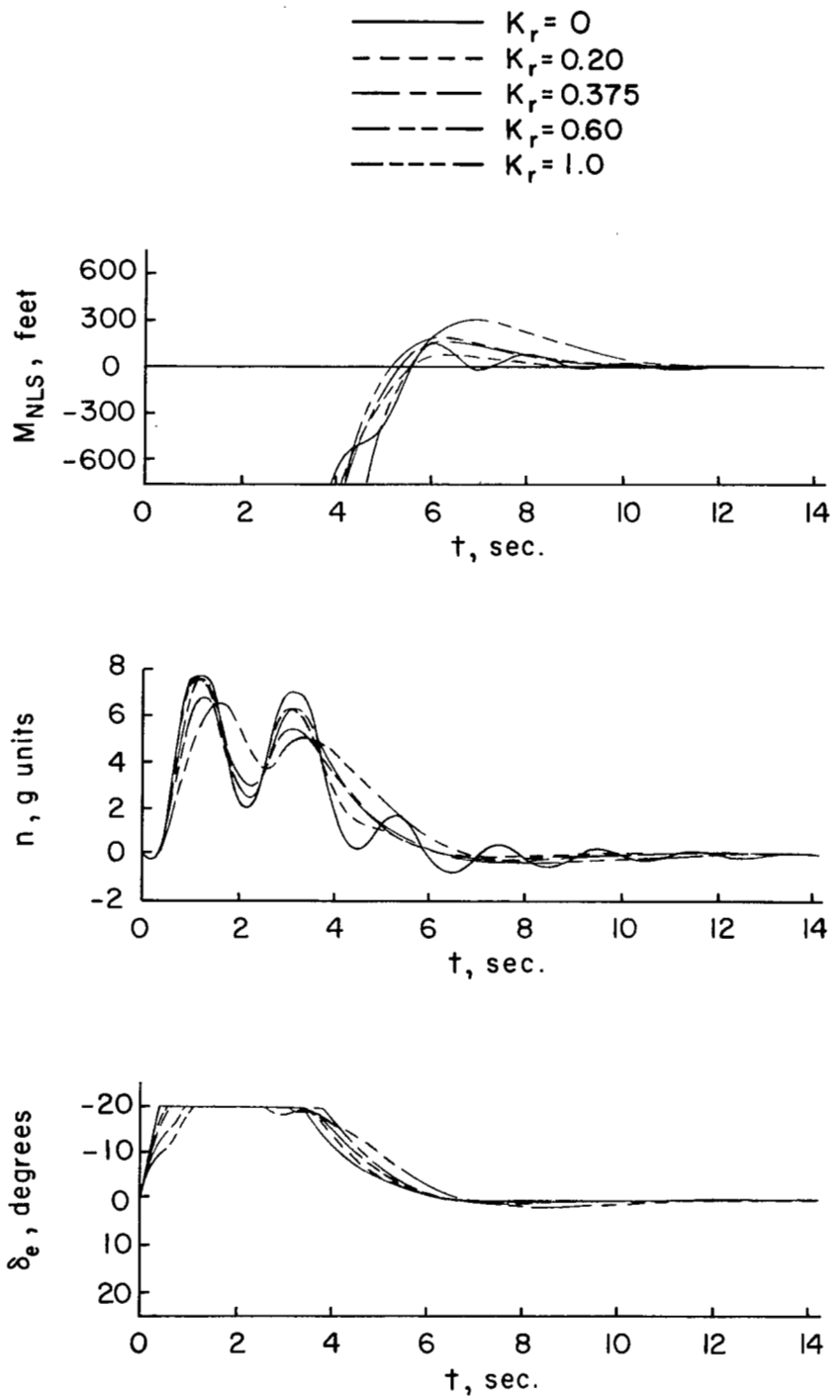

(a) $\sigma_o = 7.5^\circ$.

Figure 8.- Effect of pitch rate feedback on interceptor attack performance. K = 3.0; R_o = 60,000 feet.

[redacted]

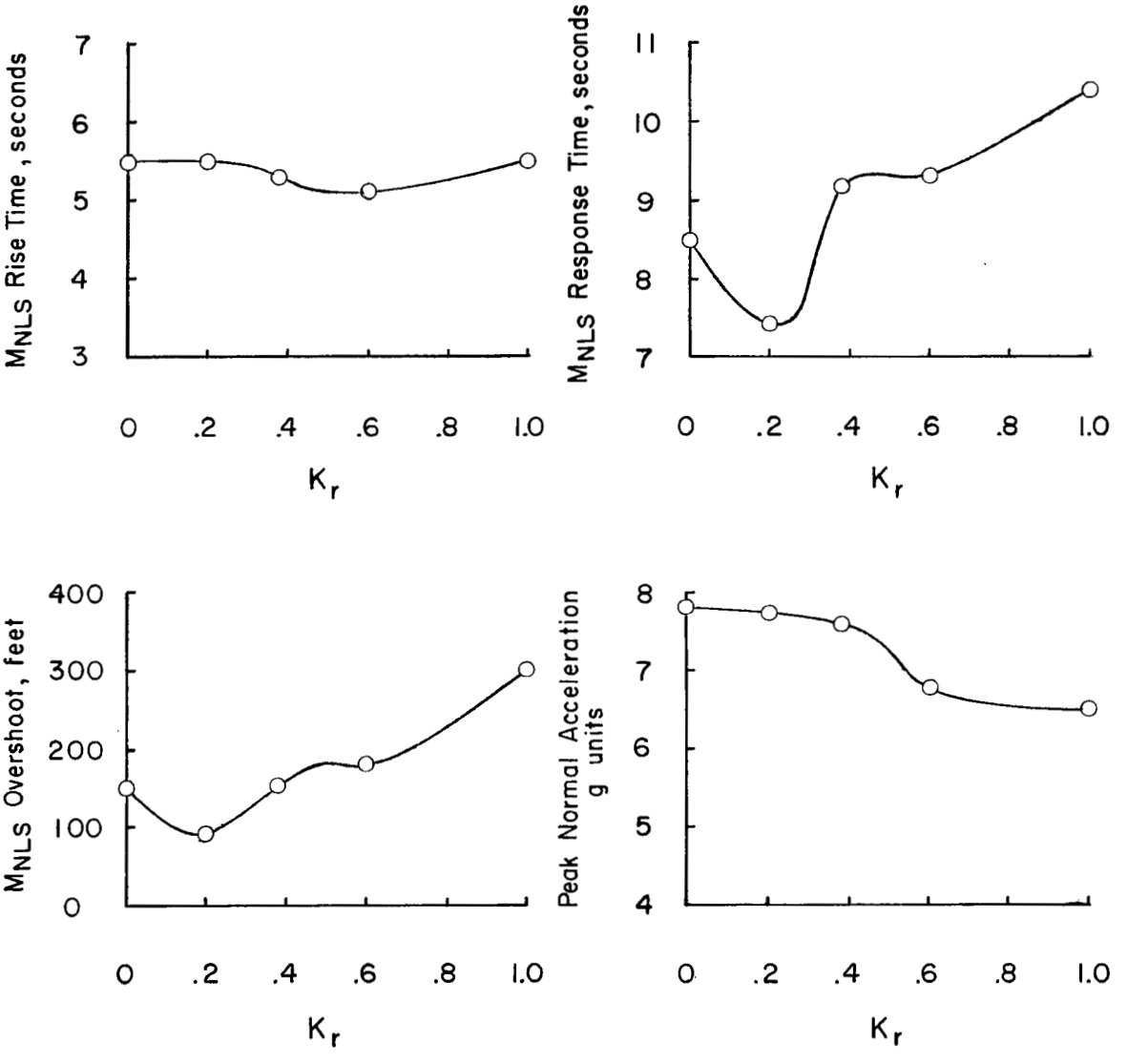

(b) Summary plots.

Figure 8.- Concluded.

[redacted]

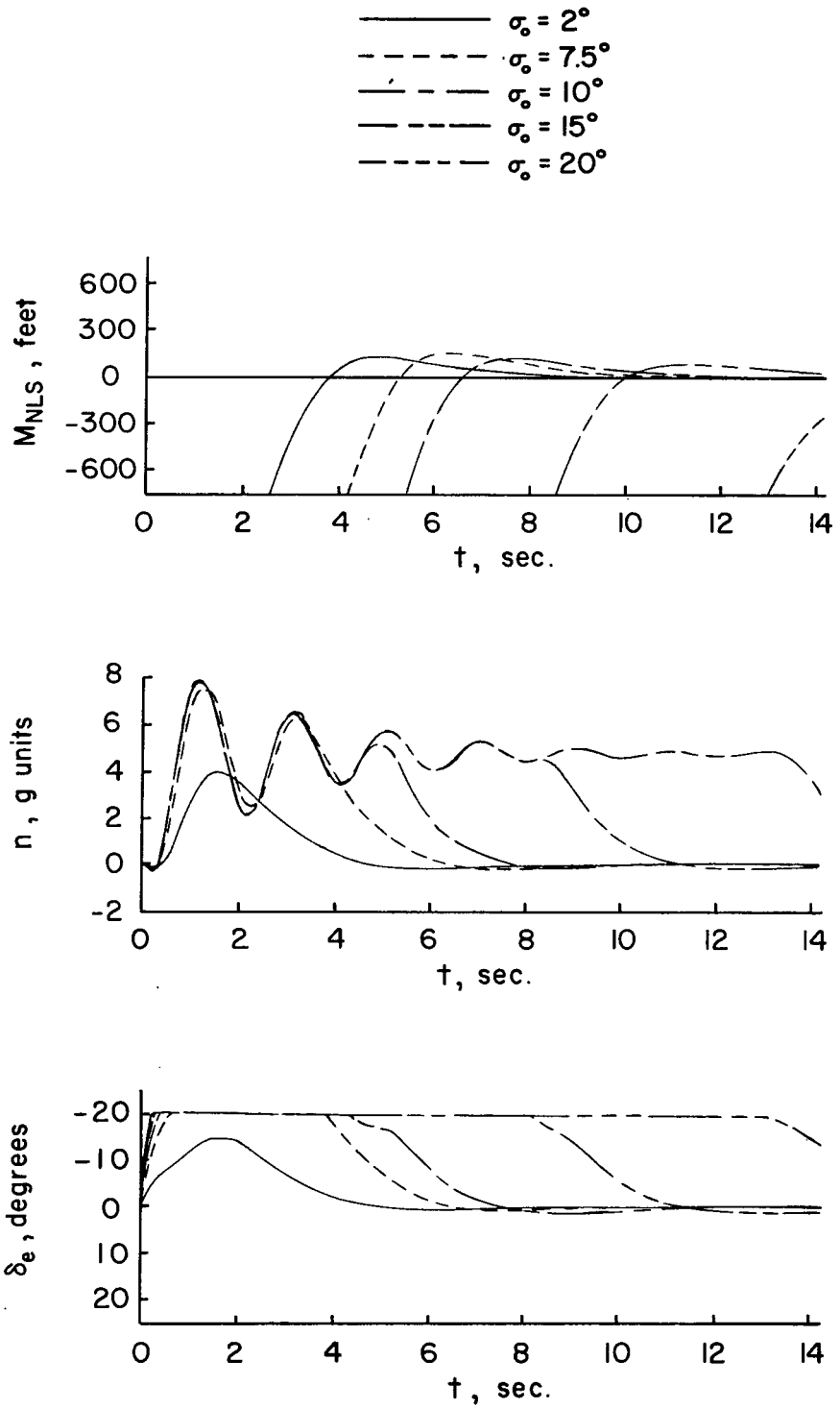

Figure 9.- Effect of initial values of radar elevation angle σ on interceptor attack performance. $K = 3.0$; $K_r = 0.375$; $R_o = 60{,}000$ feet.

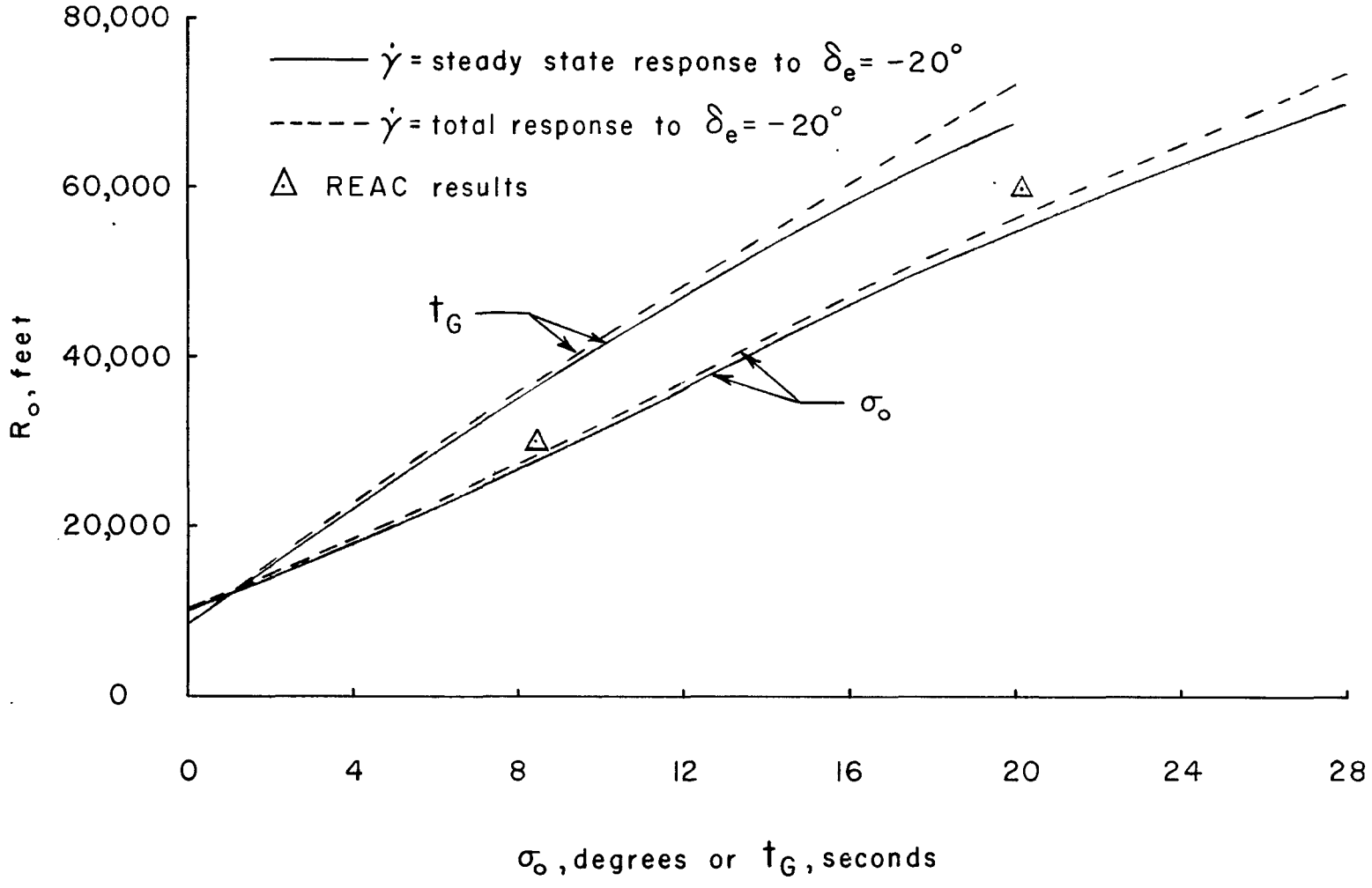

Figure 10.- Combinations of R_o, σ_o, and t_G for which a hit may be obtained in this investigation. ($\alpha_o = \theta_o = 1.9°$, $\gamma_T = \pi$.)

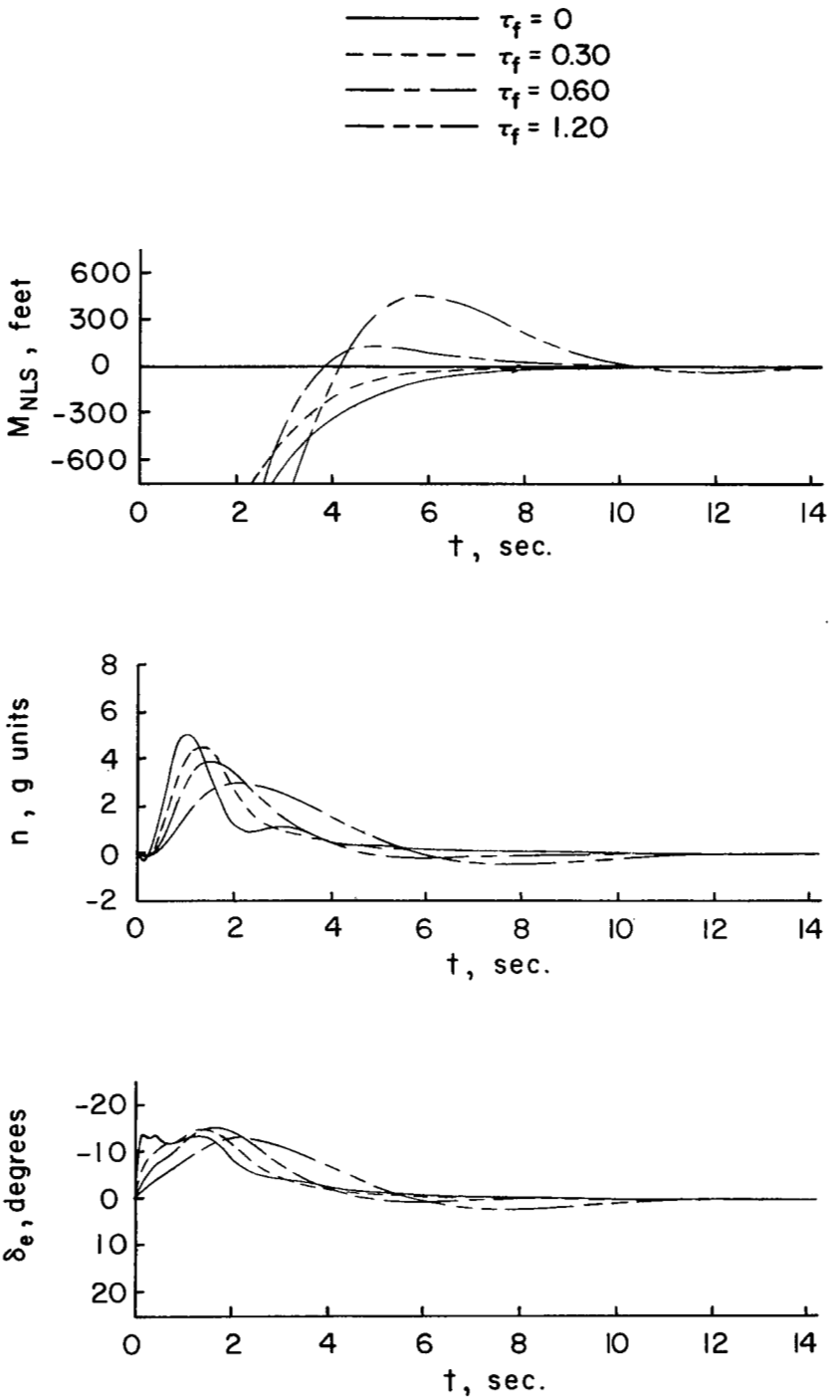

(a) $\sigma_o = 2^o$.

Figure 11.- Effect of filter-time constant τ_f on interceptor attack performance. K = 3.0; K_r = 0.375; R_o = 60,000 feet.

[redacted]

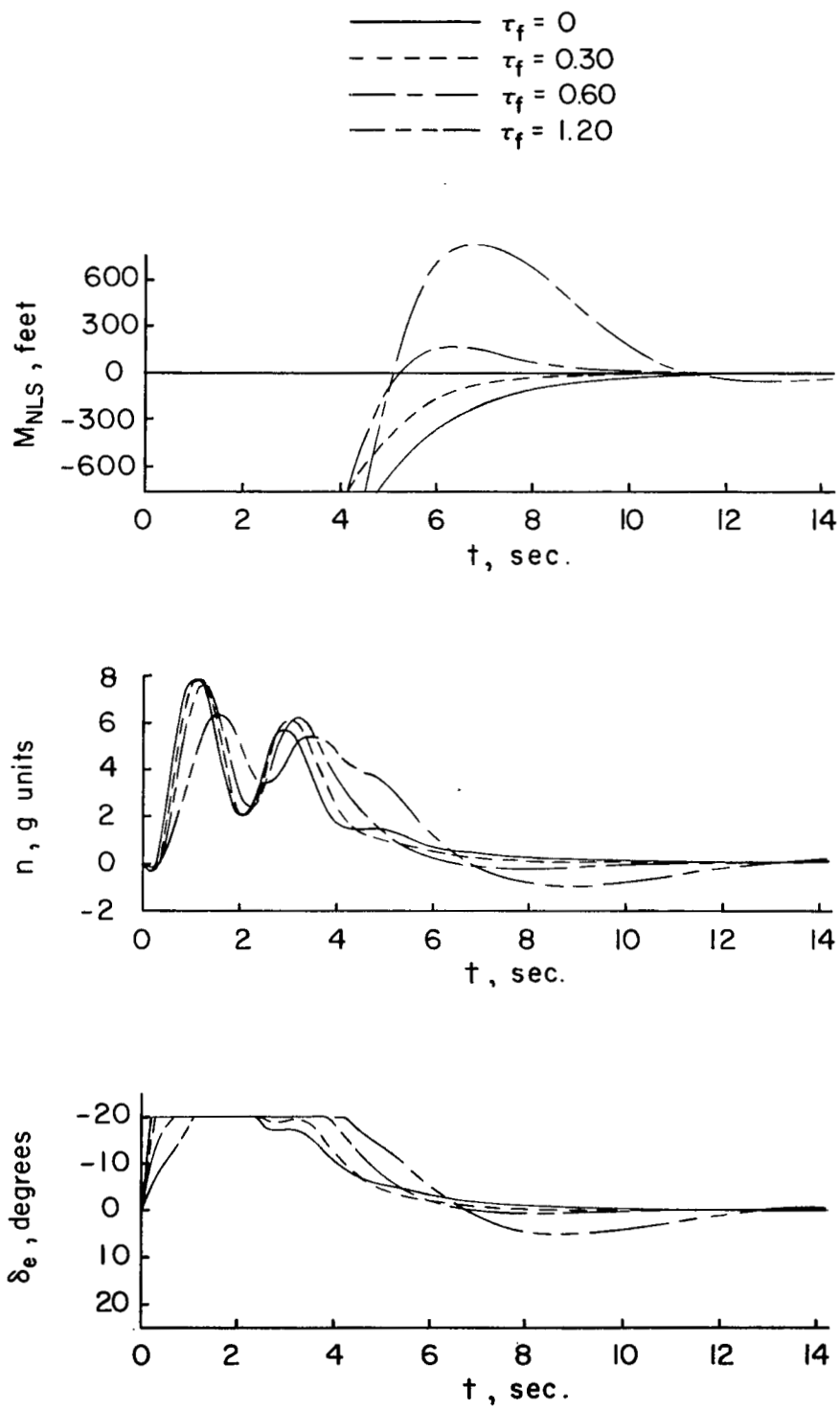

(b) $\sigma_o = 7.5^\circ$.

Figure 11.- Continued.

[redacted]

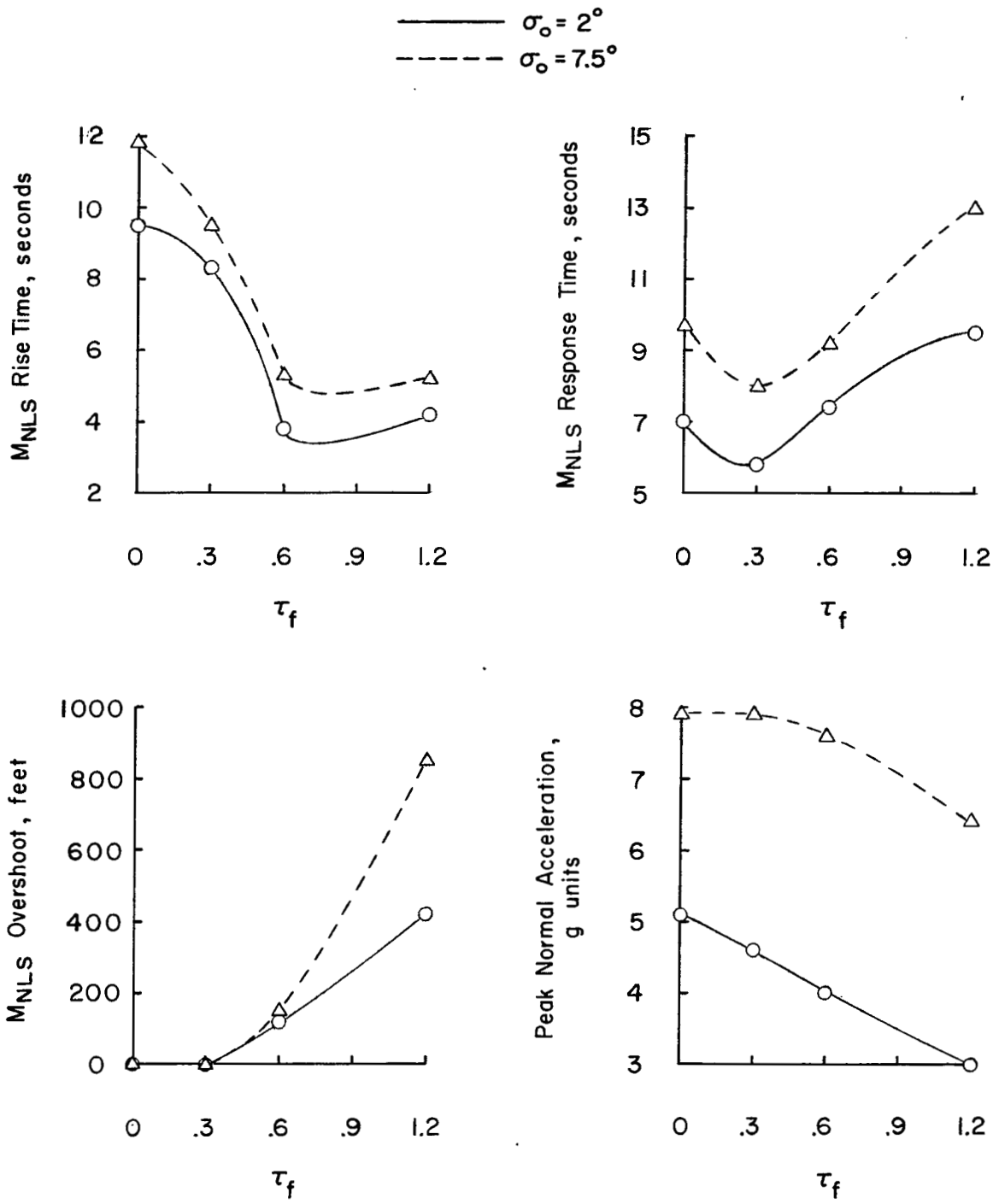

(c) Summary plots.

Figure 11.- Concluded.

[redacted]

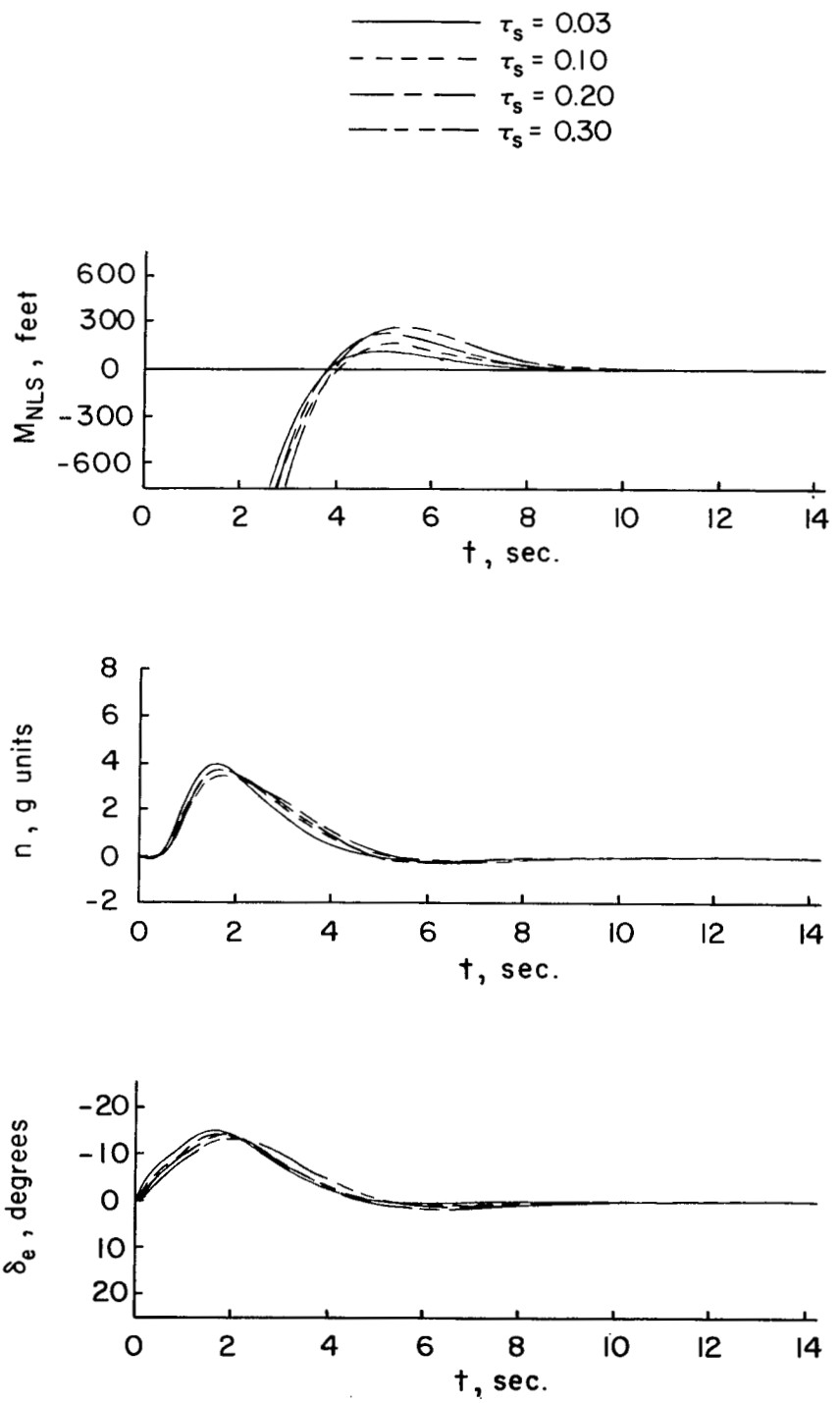

(a) $\sigma_o = 2^o$.

Figure 12.- Effect of servotime constant τ_s on interceptor attack performance. K = 3.0; K_r = 0.375; R_o = 60,000 feet.

[redacted]

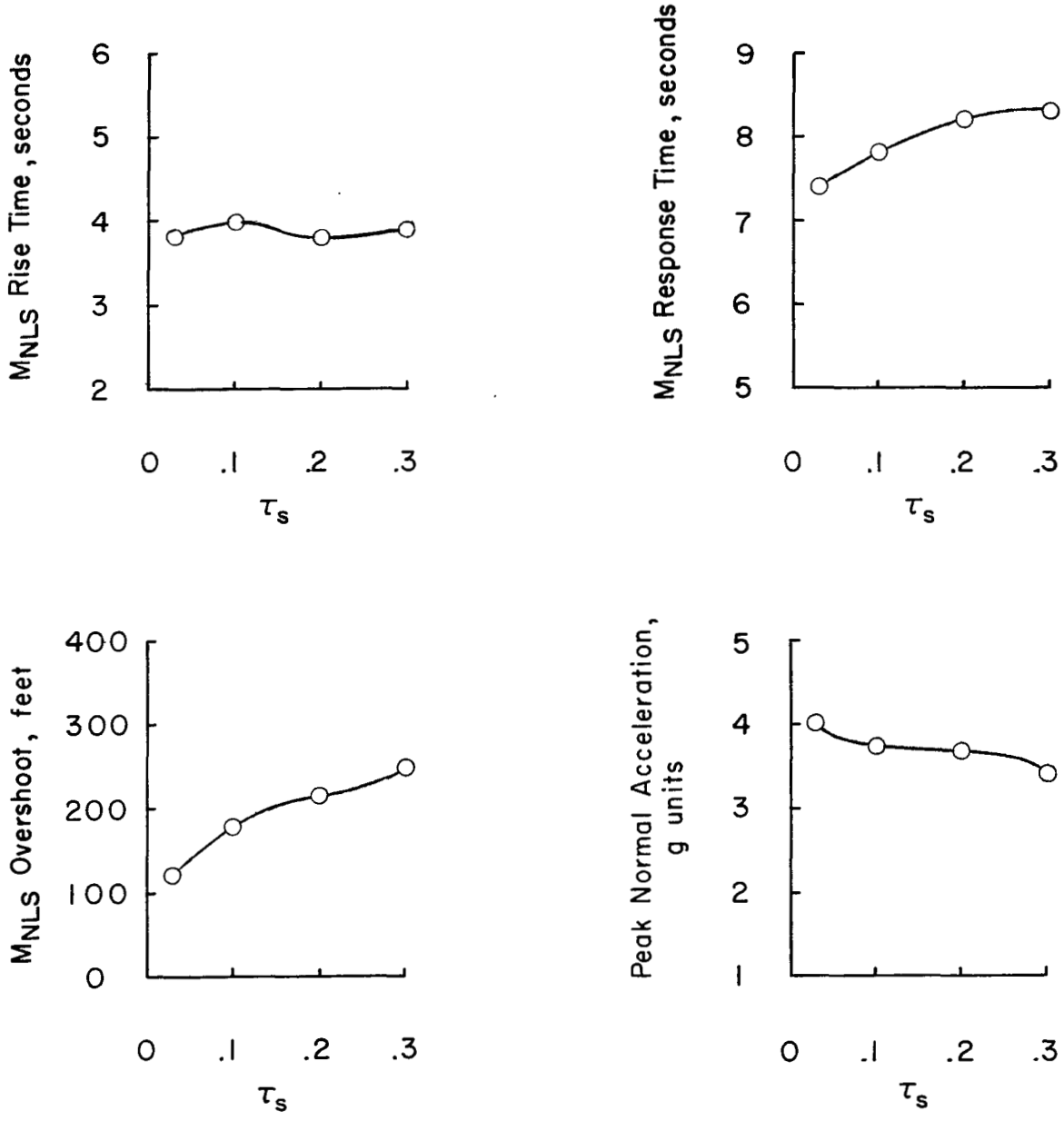

(b) Summary plots.

Figure 12.- Concluded.

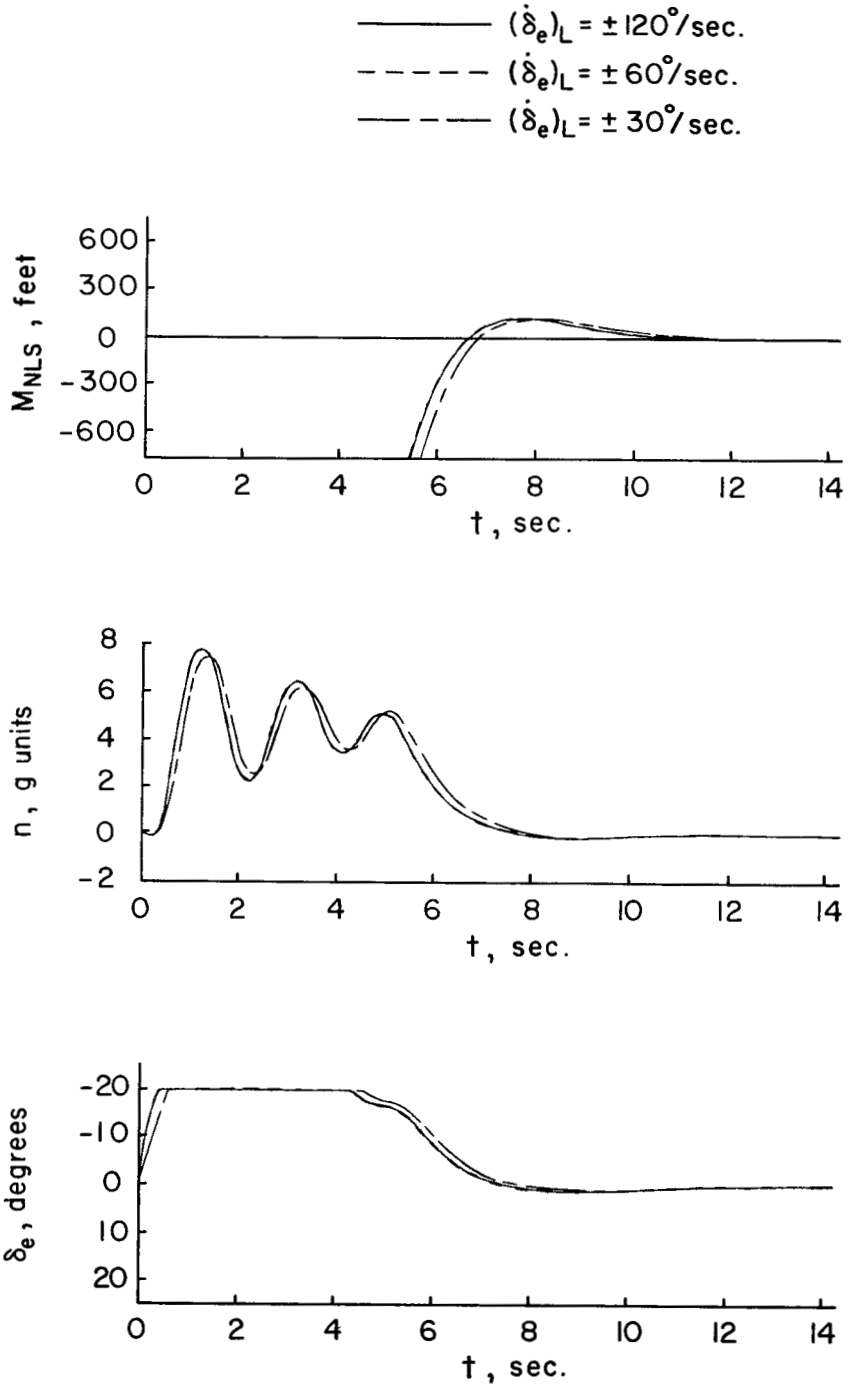

(a) $\sigma_o = 10°$.

Figure 13.- Effect of limiting rate of elevator deflection $\dot{\delta}_e$ on interceptor attack performance. $K = 3.0$; $K_r = 0.375$; $R_o = 60{,}000$ feet; $(\delta_e)_L = \pm 20°$.

[redacted]

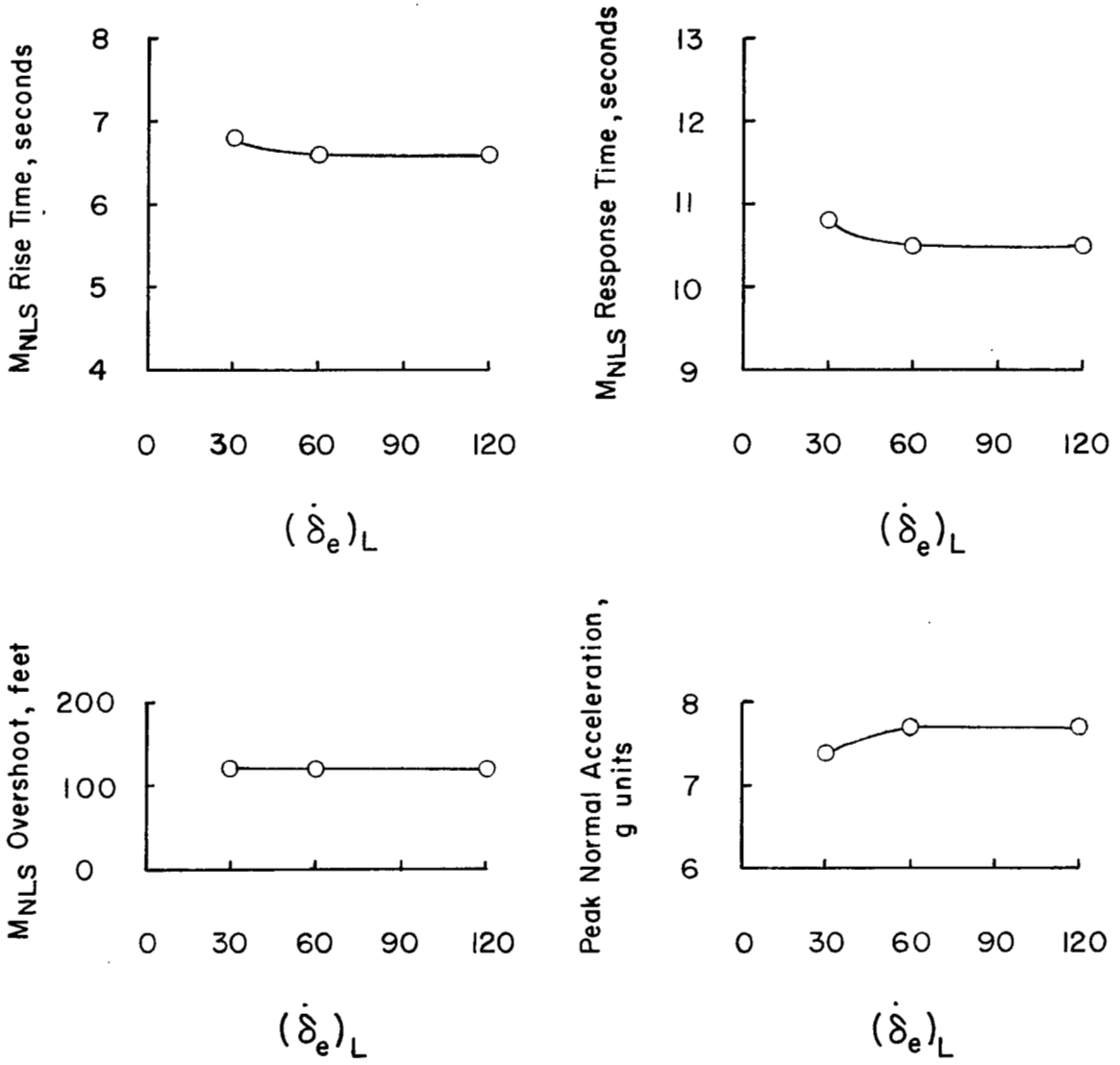

(b) Summary plots.

Figure 13.- Concluded.

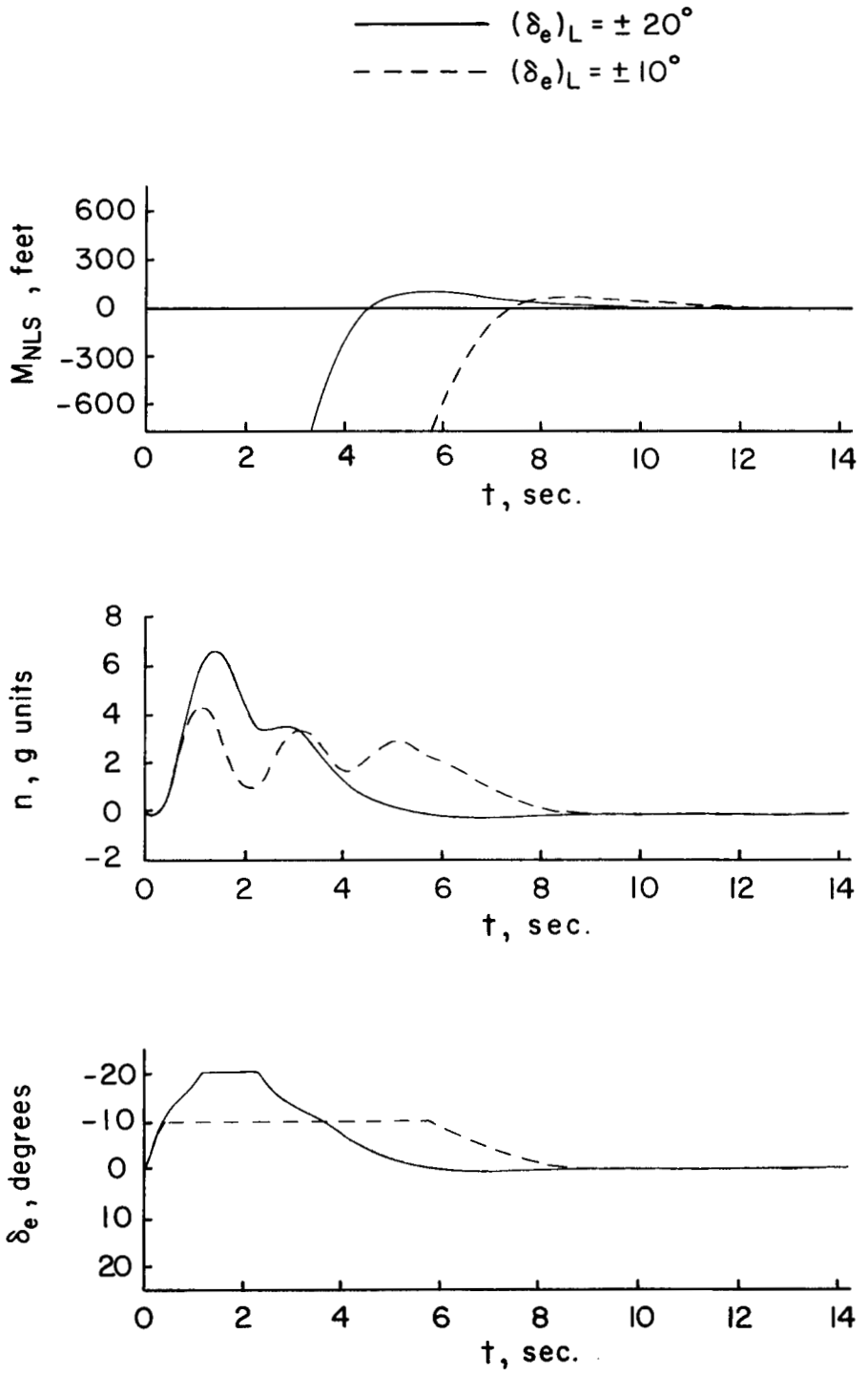

Figure 14.- Effect of limiting elevator deflection δ_e on interceptor attack performance. $K = 3.0$; $K_r = 0.375$; $R_o = 60{,}000$ feet; $\sigma_o = 5°$; $(\dot{\delta}_e)_L = \pm 120°/\text{sec}$.

[redacted]

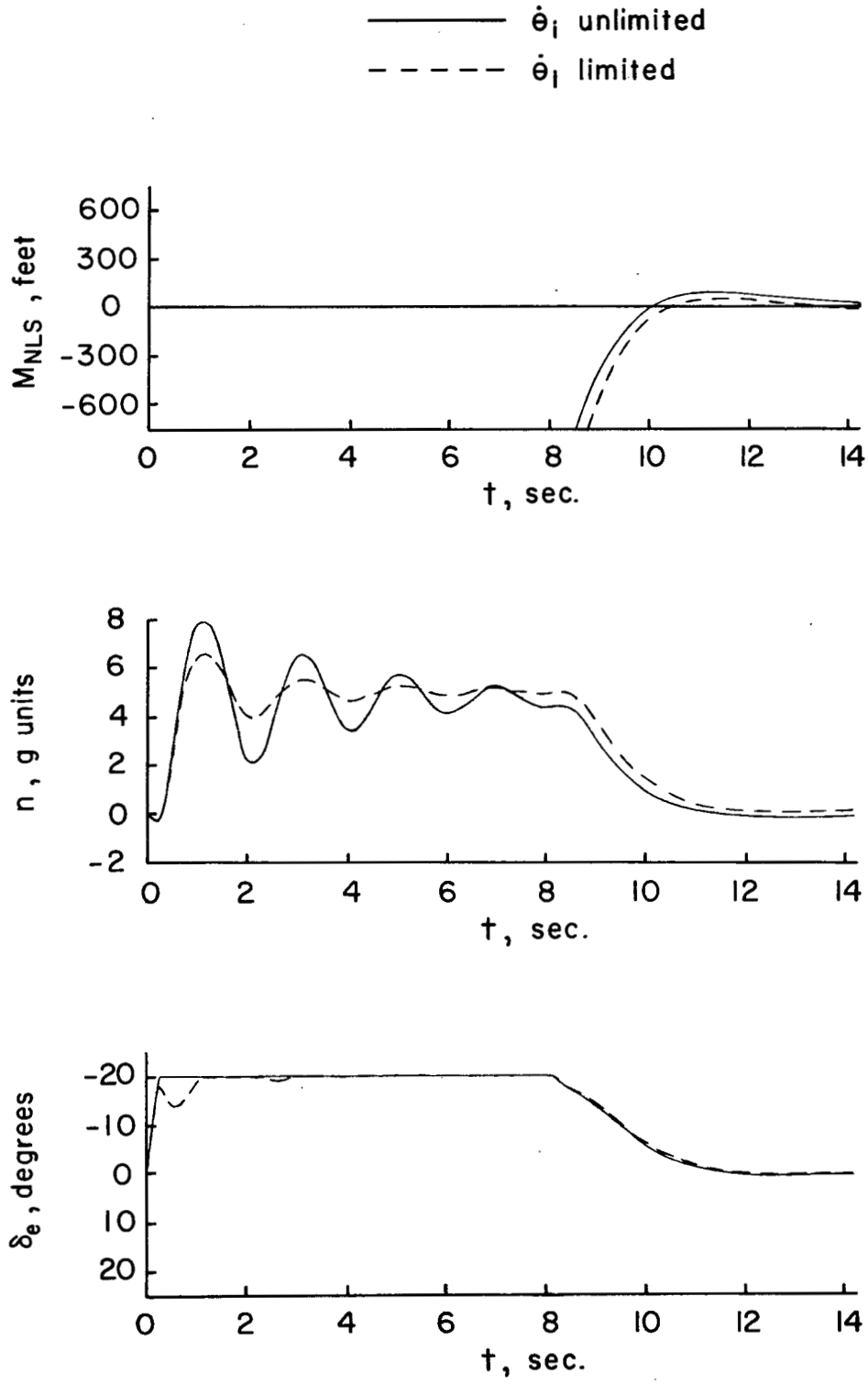

Figure 15.- Comparison of unlimited $\dot{\theta}_i$ and $\dot{\theta}_i$ limited to value required for $n_{ss} = 5$.

[redacted]

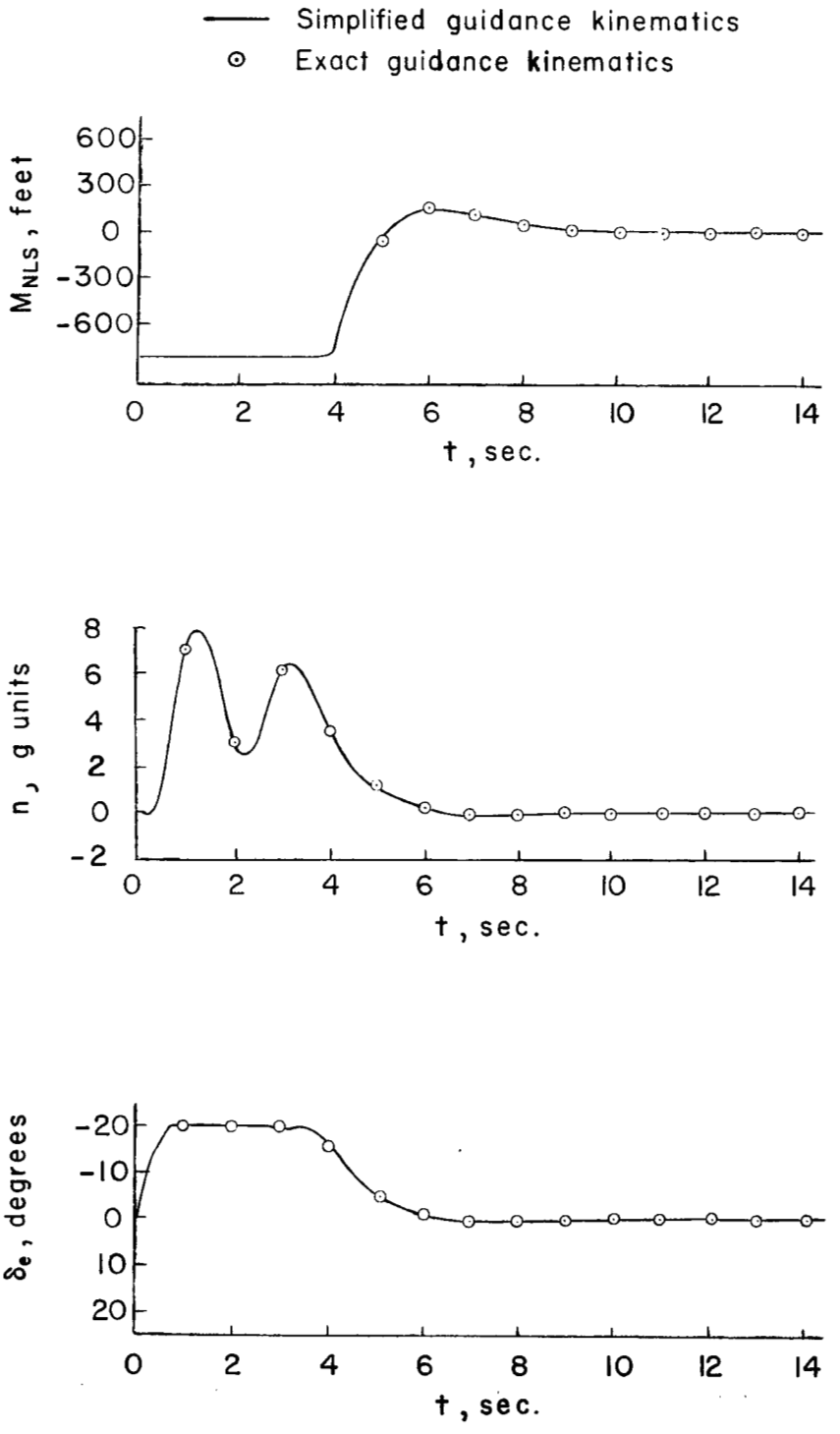

Figure 16.- Comparison of interceptor attack performance for exact and simplified guidance kinematics. $K = 3.0$; $K_r = 0.375$; $R_o = 60{,}000$ feet; $\sigma_o = 7.5^\circ$.

[redacted]

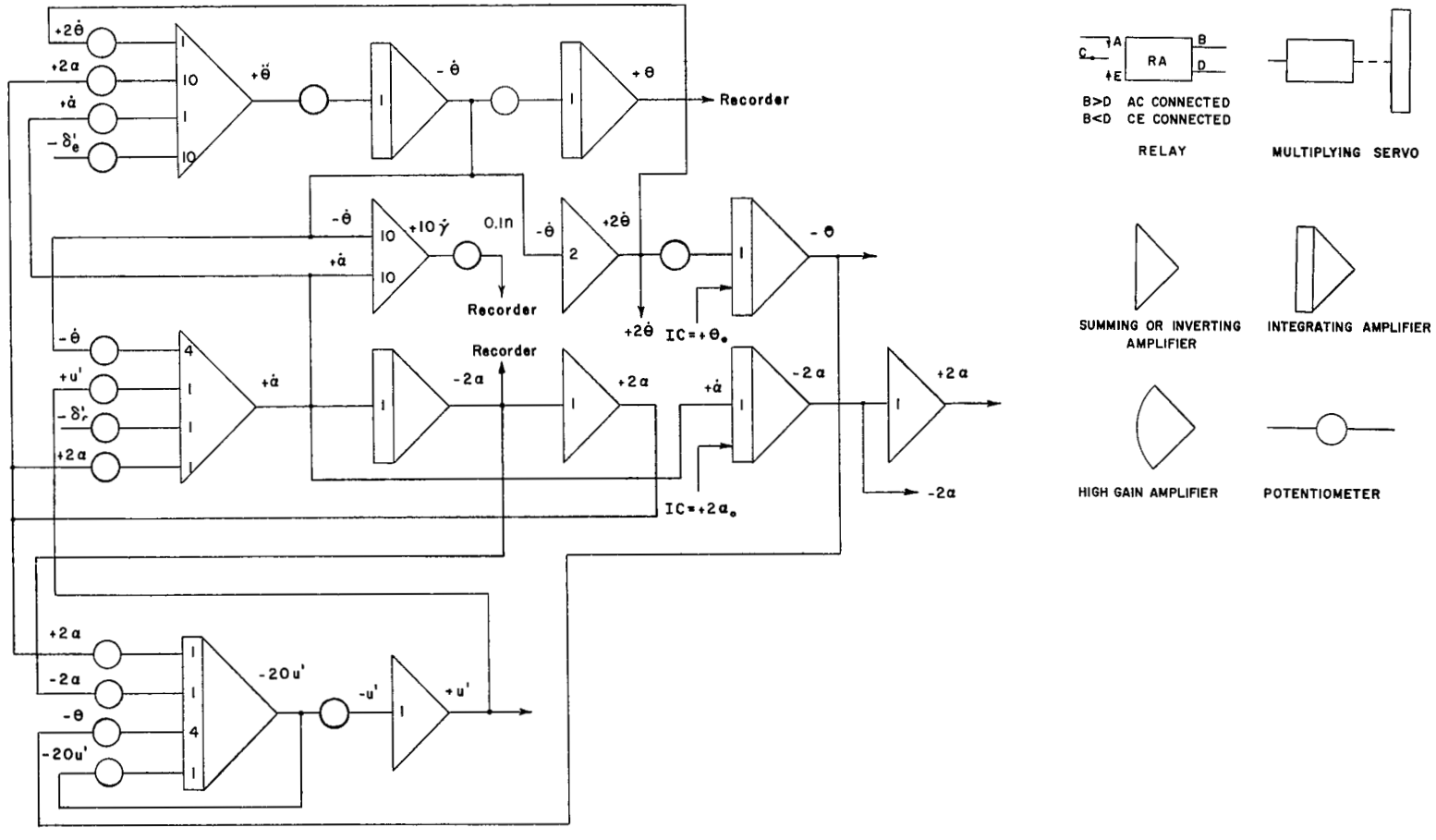

(a) Airframe equations.

Figure 17.- Analog schematic diagram of equations presented in appendix A and table of schematic symbols.

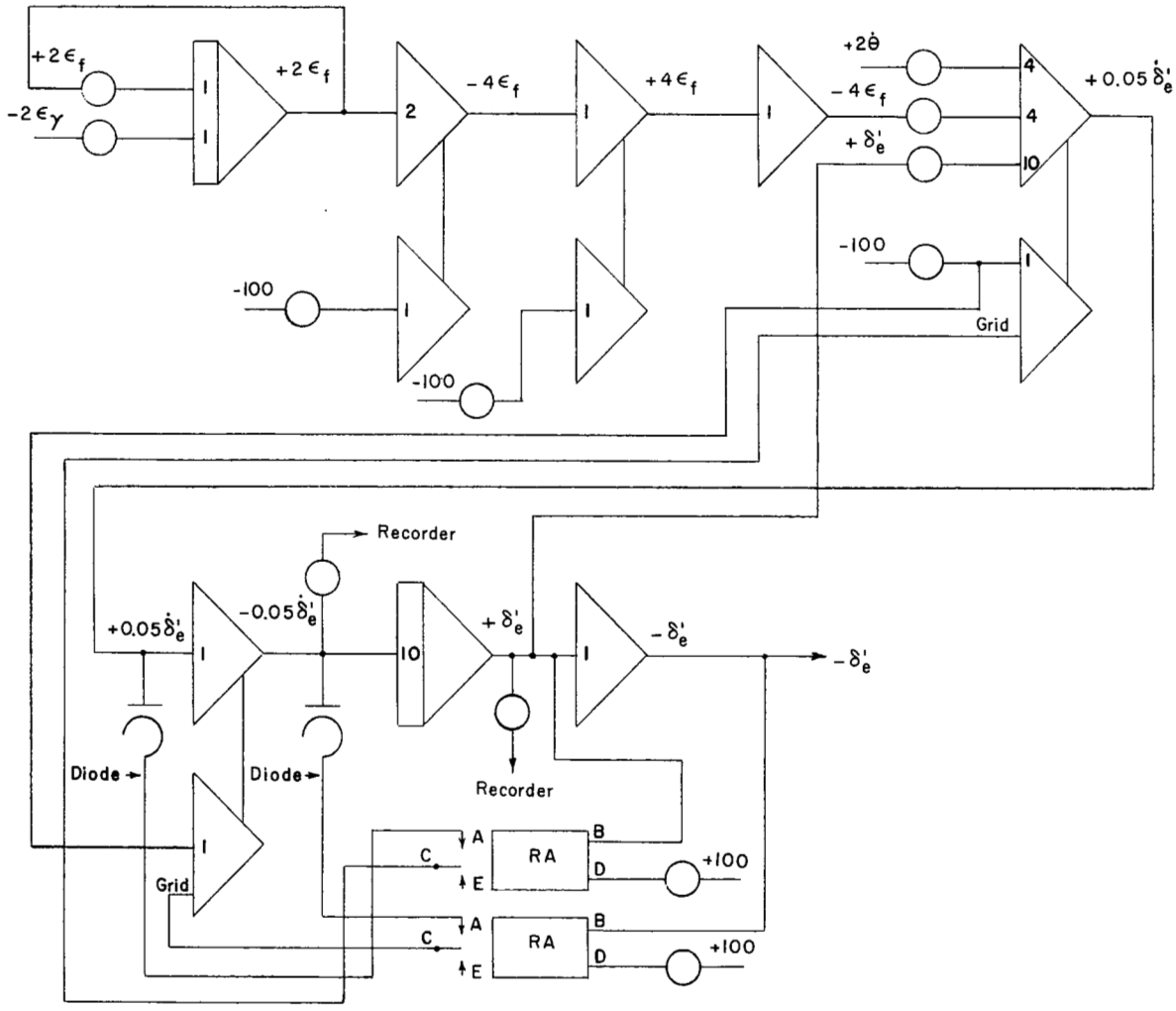

(b) Control equations.

Figure 17.- Continued.

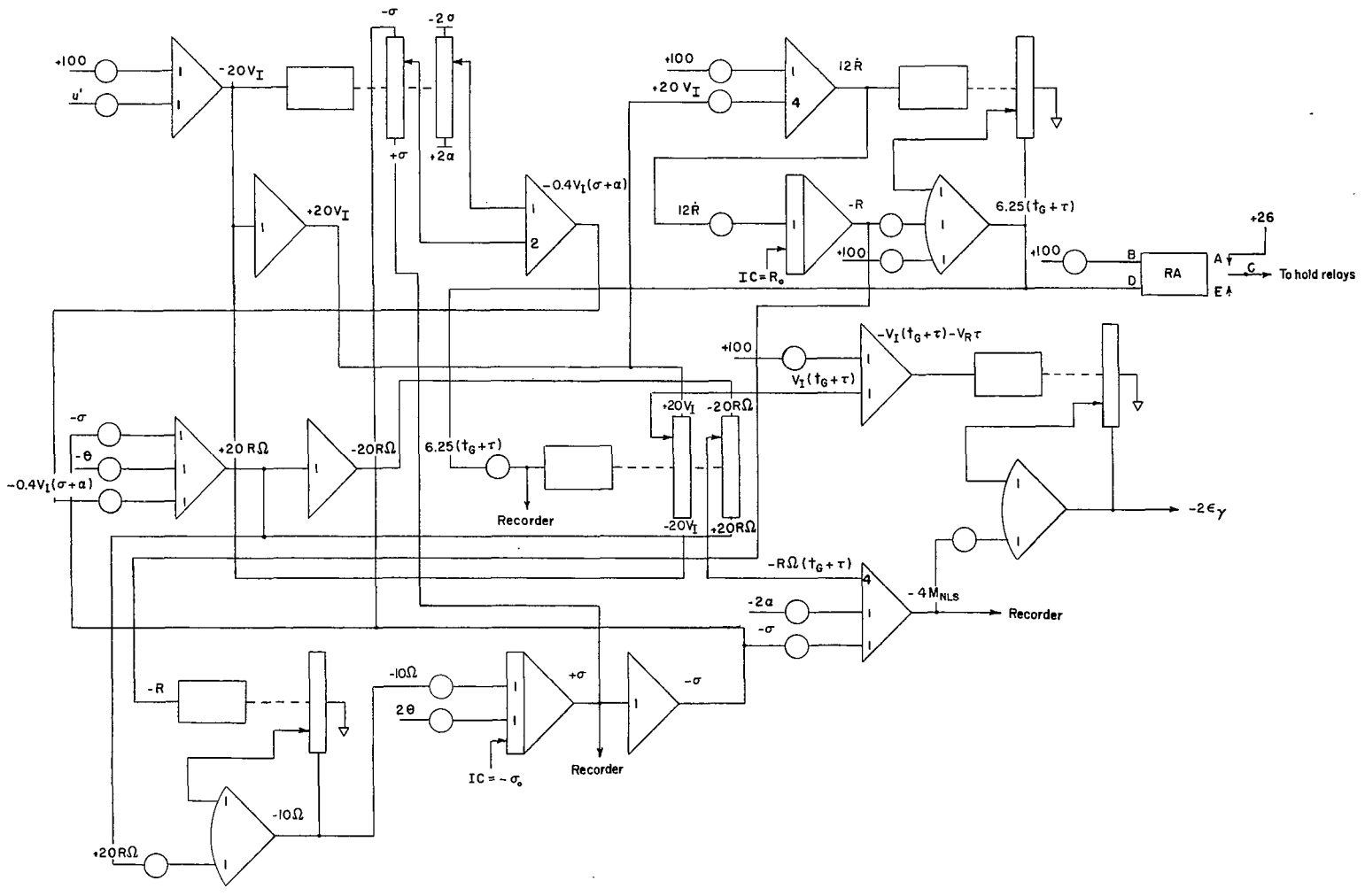

(c) Kinematic equations.

Figure 17.- Concluded.